

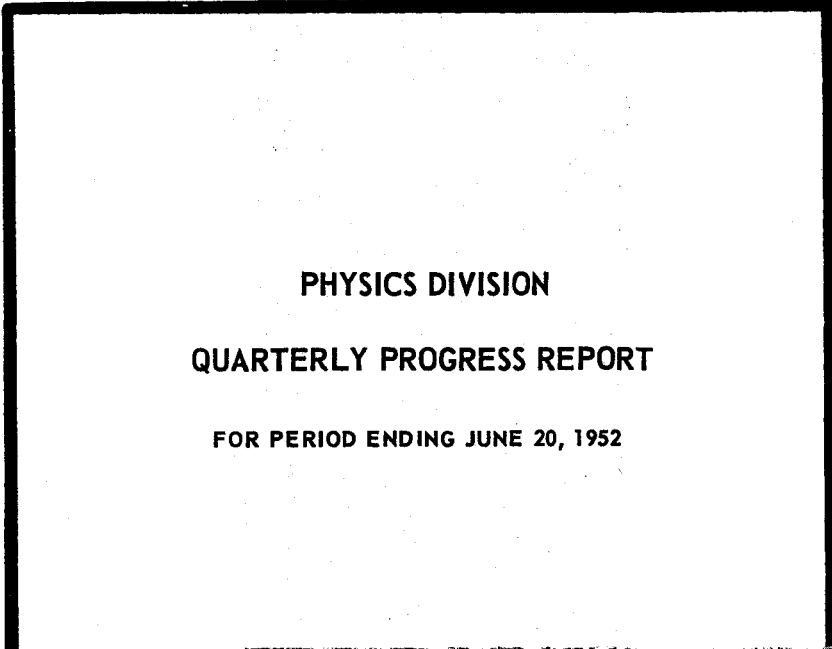


3 4456 0360600 6

ORNL-1365

Progress

54



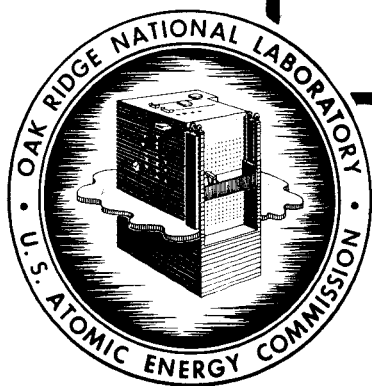
PHYSICS DIVISION
QUARTERLY PROGRESS REPORT
FOR PERIOD ENDING JUNE 20, 1952

CENTRAL RESEARCH LIBRARY
DOCUMENT COLLECTION

LIBRARY LOAN COPY

DO NOT TRANSFER TO ANOTHER PERSON

If you wish someone else to see this document,
send in name with document and the library will
arrange a loan.



OAK RIDGE NATIONAL LABORATORY
OPERATED BY
CARBIDE AND CARBON CHEMICALS COMPANY
A DIVISION OF UNION CARBIDE AND CARBON CORPORATION



POST OFFICE BOX P
OAK RIDGE, TENNESSEE

ORNL-1365

This document consists of 36 pages.
Copy **5** of 331 copies. Series A.

Contract No. W-7405-eng-26

PHYSICS DIVISION
QUARTERLY PROGRESS REPORT
for Period Ending June 20, 1952

A. H. Snell, Director
E. O. Wollan, Associate Director

DATE ISSUED

OAK RIDGE NATIONAL LABORATORY
operated by
CARBIDE AND CARBON CHEMICALS COMPANY
A Division of Union Carbide and Carbon Corporation
Post Office Box P
Oak Ridge, Tennessee



3 4456 0360600 6



INTERNAL DISTRIBUTION

- | | |
|--|-----------------------------------|
| 1. G. T. Felbeck (C&CCC) | 36. W. C. Koehler |
| 2. Biology Library | 37. W. K. Ergen |
| 3. Health Physics Library | 38. E. P. Blizard |
| 4. Metallurgy Library | 39. M. E. Rose |
| 5-6. Training School Library | 40. G. E. Boyd |
| 7. Reactor Experimental
Engineering Library | 41. Lewis Nelson |
| 8-13. Central Files | 42. R. W. Stoughton |
| 14. C. E. Center | 43. C. E. Winters |
| 15. C. E. Larson | 44. W. H. Jordan |
| 16. W. B. Humes (K-25) | 45. E. C. Campbell |
| 17. L. B. Emler (Y-12) | 46. D. S. Billington |
| 18. A. M. Weinberg | 47. M. A. Bredig |
| 19. E. H. Taylor | 48. R. S. Livingston |
| 20. E. D. Shipley | 49. C. P. Keim |
| 21. E. J. Murphy | 50. J. L. Meem |
| 22. F. C. VonderLage | 51. C. E. Clifford |
| 23. A. H. Snell | 52. G. H. Clewett |
| 24. J. A. Swartout | 53. C. D. Susano |
| 25. A. Hollaender | 54. C. J. Borkowski |
| 26. K. Z. Morgan | 55. M. J. Skinner |
| 27. F. L. Steahly | 56. L. A. Rayburn |
| 28. M. T. Kelley | 57. S. Bernstein |
| 29. E. M. King | 58. P. M. Reyling |
| 30. E. O. Wollan | 59. D. D. Cowen |
| 31. D. W. Cardwell | 60. W. M. Good |
| 32. A. S. Householder | 61. E. P. Wigner (consultant) |
| 33. L. D. Roberts | 62. H. A. Bethe (consultant) |
| 34. R. B. Briggs | 63. K. Lark-Horovitz (consultant) |
| 35. R. N. Lyon | 64. Eugene Guth (consultant) |
| | 65. J. G. Daunt (consultant) |

EXTERNAL DISTRIBUTION

66. L. C. Biedenharn, Sloans Physics Laboratory
67. R. F. Bacher, California Institute of Technology
- 68-69. Ohio State University, Attn: Professor of Naval Science
70. John Dunning, Columbia University
71. Phillips Petroleum Co., Attn: Librarian
72. R. L. Heath, American Cyanamid Co.
73. S. DeBenedetti, Carnegie Institute of Technology
74. Massachusetts Institute of Technology, Department of Electrical Engineering
75. A. von Hippel, Laboratory for Insulation Research, MIT
76. M. Goodrich, Louisiana State University
- 77-331. Given distribution as shown in TID 4500 under Physics Category

Physics Division quarterly progress reports previously issued in this series are as follows:

ORNL-325 Supplement	December, January, and February, 1948-1949
ORNL-366	Period Ending June 15, 1949
ORNL-481	Period Ending September 25, 1949
ORNL-577	Period Ending December 15, 1949
ORNL-694	Period Ending March 15, 1950
ORNL-782	Period Ending June 15, 1950
ORNL-865	Period Ending September 20, 1950
ORNL-940	Period Ending December 20, 1950
ORNL-1005	Period Ending March 20, 1951
ORNL-1092	Period Ending June 20, 1951
ORNL-1164	Period Ending September 20, 1951
ORNL-1278	Period Ending December 20, 1951
ORNL-1289	Period Ending March 20, 1952

CONTENTS

	Page
SUMMARY	1
1. HIGH-VOLTAGE PHYSICS	1
Total Neutron Cross Sections of N^{14} , Ge, Se, Cd, and Hg	1
Energy Spectra of Particles from the Reactions $He^3(Li^6, Li^5)He^4$ and $He^3(Li^6, Be^8)H^1$	2
2. RADIOACTIVITY AND NUCLEAR ISOMERISM	4
Absorption of Gamma Rays	4
Lifetime of an Excited State of Hf^{176}	6
Gamma-Gamma Angular Correlation in Ta^{181}	8
Angular Correlation of Gamma Rays	9
Short-Period Activities	9
3. LOW-TEMPERATURE PHYSICS	10
Electrical Resistance of High-Purity Zirconium Below $300^\circ K$	10
Paramagnetism of Trivalent Uranium	12
4. HEAVY-ION PHYSICS	14
Average Energy per Ion Pair	14
5. NEUTRON CROSS SECTIONS	15
Neutron Cross-Section Measurements for Polycrystalline Nickel and Nickel Oxide in the Thermal Energy Region	15
6. INSTRUMENTATION	25
Crystal Diodes	25
Neutron-Sensitive Scintillation Phosphors	25
7. THEORETICAL PHYSICS	26
The Parameterization of Quantum Electrodynamics	26



PUBLICATIONS

The following papers by members of the Physics Division appeared in open publications during the last quarter:

J. M. Blatt and L. C. Biedenharn, "Neutron-Proton Scattering with Spin-Orbit Coupling. I. General Expressions," *Phys. Rev.* **86**, 399 (1952).

G. B. Arfken, E. D. Klema, and F. K. McGowan, "Gamma-Gamma Angular Correlation in Pd¹⁰⁶," *Phys. Rev.* **86**, 413 (1952).

M. E. Rose and T. A. Welton, "The Virial Theorem for a Dirac Particle," *Phys. Rev.* **86**, 432 (1952).

G. B. Arfken, L. C. Biedenharn, and M. E. Rose, "Angular Correlation of First and Third Gamma-Rays," *Phys. Rev.* **86**, 761 (1952).

G. G. Kelley, "Pulse Amplitude Analyzers for Spectrometry," *Nucleonics* **10**, No. 4, 34 (1952).

ANNOUNCEMENTS

The following personnel have been added to the staff of the Physics Division during this quarter: P. E. F. Thurlow (velocity selector group); G. T. Chapman, J. M. Miller, F. N. Watson, and T. Love (shielding program); R. L. Macklin (high-voltage group); E. L. Zimmerman (transferred from isotope research and production to critical-experiments program).

Terminations for this period were as follows: G. P. Robinson (high-voltage group); M. C. Marney (shielding program); N. D. Young (critical-experiments program).

The research participants who will spend the summer in the Physics Division include: H. Q. Fuller, University of Missouri School of Mines, M. Goodrich, Louisiana State University, and D. S. Hughes, University of Texas (scintillation spectrometer program); R. A. Erickson, University of Tennessee, and C. C. Sartain, University of Alabama (low-temperature studies); R. R. Carlson, State University of Iowa, and J. R. Risser, Rice Institute (high-voltage studies); N. S. Gingrich, University of Missouri, and E. J. Lanterman, North Carolina State College (neutron-diffraction studies); R. C. Keen, University of Alabama (ANP critical experiments); D. E. Matthews, University of Mississippi (neutron cross-sections program); C. A. Randall, Ohio State University (instrument development).

The following consultants will be spending part of the summer with the theoretical group: J. M. Jauch, State University of Iowa; G. Goertzel, New York University; and E. Greuling, Duke University.

Undergraduate students working in the Physics Division this summer are: M. E. Miles, Cornell University (low-temperature studies); J. E. Russell, Yale University (high-voltage group).

PHYSICS DIVISION QUARTERLY PROGRESS REPORT

SUMMARY

High-Voltage Physics. The total neutron cross section measurements of N^{14} have been extended from 1.7 to 4.0 Mev by use of the $H^3(p,n)He^3$ neutron source on the 5-Mev Van de Graaff. Five resonances were resolved in this energy interval. Total average neutron cross sections of Ge, Se, Cd, and Hg were also measured from 0.4 to 3.5 Mev.

The energy spectrum of the particles from the reactions $He^3(Li^6, Li^5)He^4$ and $He^3(Li^6, Be^8)H^1$ has been observed at the 360-kev He^3 energy obtained with the Cockcroft-Walton accelerator. The data indicate an excited state of Be^8 , 2.05 Mev above the ground state.

Radioactivity and Nuclear Isomerism. Accurate measurements of the absorption coefficients of four monoenergetic gamma rays in lead and aluminum are reported. The need for better measurements on coherent-scattering cross sections is apparent, and such measurements are now being made.

The decay scheme for Hf^{181} is reported. The dependence of the angular correlation upon the chemical state of the atom is of particular interest.

A new isomer with a half life of about 0.35 s has been found in germanium.

Low-Temperature Physics. Electrical resistance as a function of temperature has been measured for a high-purity zirconium sample from 14 to 300°K, and the Debye θ has been calculated from the temperature-dependence of the resistance.

A solid solution of uranium trifluoride in lanthanum chloride has been prepared and found to be paramagnetic in the liquid-helium temperature region.

Heavy-Ion Physics. A discussion is given of proposed techniques for measuring the number of electron volts per ion pair in gases as a function of the energy of the ionizing particles.

Neutron Cross Sections. The transmission cross sections of powdered nickel and nickel oxide have been measured with a crystal spectrometer in the very low energy range, including the first and several succeeding Bragg discontinuities. The beam incident on the crystal was first totally reflected from a glass mirror to eliminate higher order reflections from the crystal. The coherent cross sections and the energy-dependence of the thermal diffuse scattering were determined; the latter finding is compared with theory.

Instrumentation. A much-improved neutron-sensitive phosphor has been discovered in europium-activated lithium iodide. A resolution of 5% at 4.8 Mev is now possible.

A study of commercially available germanium diodes shows that the majority are unsuitable in high-speed electronic circuits when quick recovery is required.

Theoretical Physics. The formalism relating to the parameterization of quantum electrodynamics has been extended.

1. HIGH-VOLTAGE PHYSICS

TOTAL NEUTRON CROSS SECTIONS OF N^{14} , Ge, Se, Cd, AND Hg

C. H. Johnson	J. K. Bair
H. B. Willard	J. D. Kington

Measurements of the total cross section of nitrogen have been extended from 1.7 to 4.0 Mev by means of a simple transmission experiment. Scattering samples containing nitrogen⁽¹⁾ were formed

⁽¹⁾Samples were made of aminotetrazole and carbon as described by C. H. Johnson, B. Petree, and R. K. Adair, *Phys. Rev.* 84, 775 (1951).

in thin-walled cylinders 3 cm in diameter. Neutrons were produced by bombarding a tritium gas target with protons from the 5-Mev Van de Graaff and were detected by means of a propane recoil counter placed at 0 deg to the proton beam and 25 cm from the neutron source. The neutron flux was monitored by a long counter placed at 30 deg to the beam. The transmission of the nitrogen was determined by interposing the samples midway between source and detector. In this geometry, 1.6% of the neutrons scattered by the nitrogen will reach the detector if the scattering is isotropic. No correction was

HIGH-VOLTAGE PHYSICS

made for this scattering-in. The background intensity of neutrons scattered into the detector from the walls and floors was measured by interposing a paraffin cone between source and detector. Backgrounds measured in this manner were less than 1% and were neglected.

Figure 1.1 shows the total cross section of nitrogen as a function of neutron energy. Vertical heights of the symbols represent standard statistical deviation of data points. A correction has been applied to the neutron energy for the stopping power of the tritium gas target and the 0.0002-in. entrance foil to the target. This correction was determined experimentally by observing the shift of the 1.12- and 1.60-Mev resonances⁽²⁾ and was extrapolated to higher energies by using stopping-power curves.⁽³⁾ The resulting uncertainty in neutron energy is 50 kev. A spread in the neutron energy results primarily from the nonuniformity in the aluminum foil; this spread was found to be

(2) J. J. Hinchley, P. H. Stelson, and W. M. Preston, *Phys. Rev.* 86, 483 (1952).

(3) M. S. Livingston and H. A. Bethe, *Revs. Modern Phys.* 9, 245 (1937).

35 kev by observing the apparent width of the narrow 1.12- and 1.60-Mev resonances.

Figure 1.2 shows the total cross sections of four heavier elements, Ge, Se, Cd, and Hg, in the energy region from 0.4 to 3.5 Mev. These were measured in the same manner as that described in the foregoing material, except that the center of the counter was 40 cm from the target. In this geometry the scattering-in correction for isotropic scattering is 0.5%; no scattering-in correction was applied. The four curves in Fig. 1.2 fit smoothly on the three-dimensional, total cross-section surface given by Barschall.⁽⁴⁾

ENERGY SPECTRA OF PARTICLES FROM THE REACTIONS $\text{He}^3(\text{Li}^6, \text{Li}^5)\text{He}^4$ AND $\text{He}^3(\text{Li}^6, \text{Be}^8)\text{H}^1$

W. M. Good W. E. Kunz
C. D. Moak

A separated Li^6 target has been bombarded with He^{3++} ions, in the target arrangement previously

(4) H. H. Barschall, *Phys. Rev.* 86, 431 (1952).

UNCLASSIFIED
DWG.15770

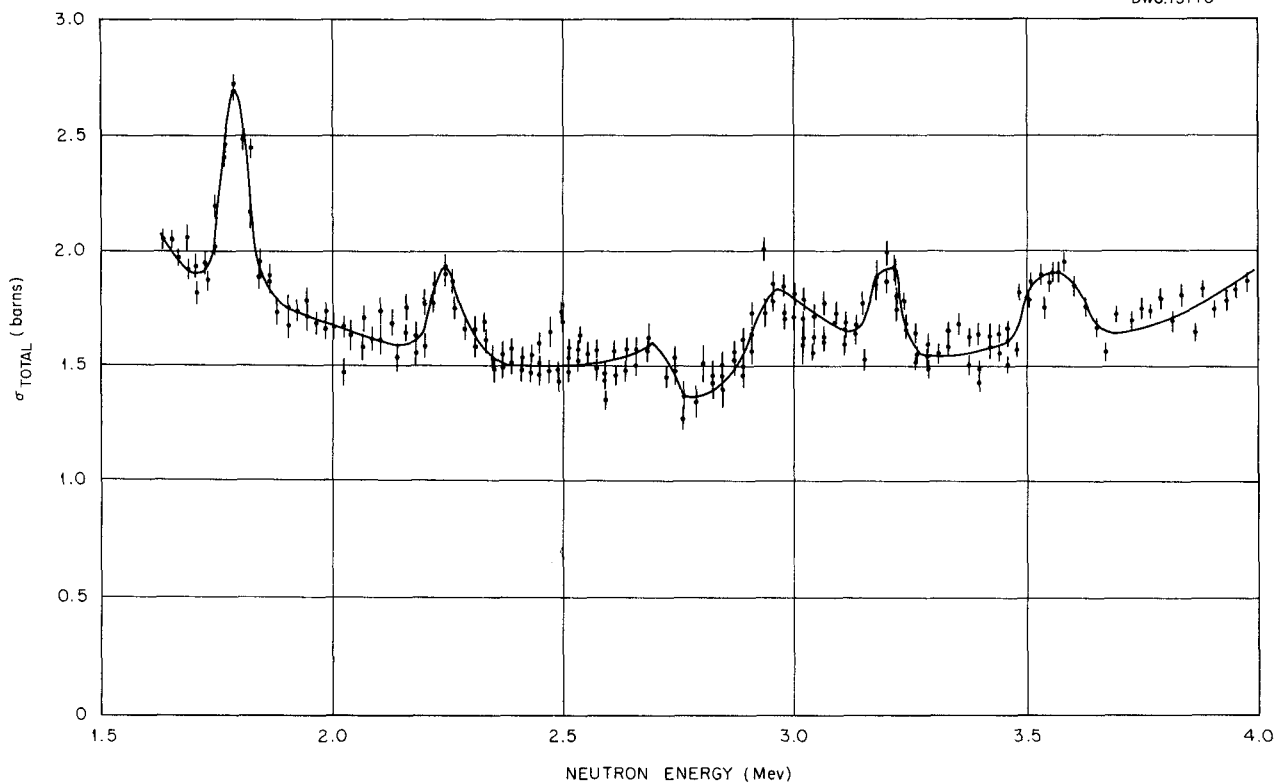


Fig. 1.1. Total Cross Section of N^{14} (Resolution, 35 kev).

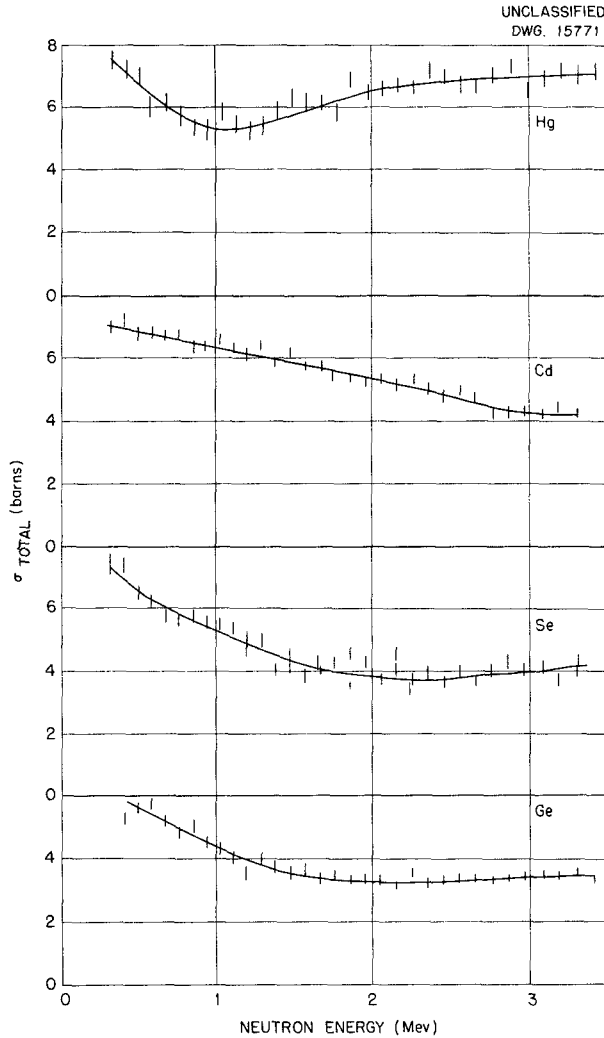
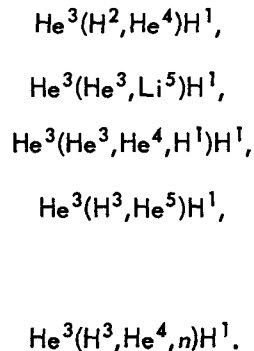


Fig. 1.2. Total Cross Sections of Hg, Cd, Se, and Ge.

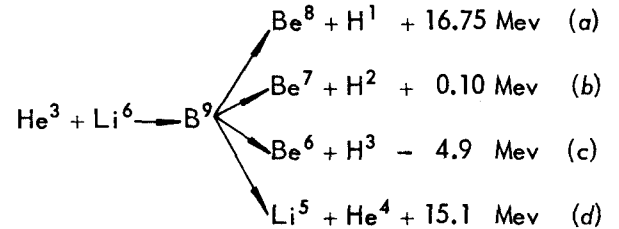
described,⁽⁵⁾ for study of the energy spectra of particles from the reactions



⁽⁵⁾C. D. Moak and W. M. Good, *Physics Division Quarterly Progress Report for Period Ending March 20, 1952, ORNL-1289, p. 4.*

The target was in the form of Li_2SO_4 fused on a platinum backing and was heated in vacuum to break up the water of crystallization.

The compound-state nucleus, B^9 , can break up into the following modes:



Reaction (a) would provide a means of studying levels in Be^8 .

A preliminary attempt to observe the reactions at 360 keV with He^{3+} revealed mode (d). However, mode (a) was largely obscured by the impurity reaction $\text{He}^3(\text{H}^2, \text{He}^4)\text{H}^1$. It had been found that the ion source delivered about $0.05 \mu\text{a}$ of He^{3++} ions, and with these ions and the 360-keV generator voltage a reasonable counting rate was observed when the He^{3++} beam was allowed to strike the Li^6 target.

The energy spectrum of particles resulting from the bombardment of Li^6 by He^3 is shown in Fig. 1.3. The impurity reaction $\text{He}^3(\text{H}^2, \text{He}^4)\text{H}^1$ at 320 keV served to give a calibration that was obtained at the beginning and at the end of the run. A drift of the order of 1% is seen to have occurred. The higher energy peak yields a value of Q of 17.35 MeV based upon the impurity peak as a calibration. This checks to within 3% of that expected from mass values. The lower energy peak gives $Q = 15.3 \pm 0.4$ MeV. This would indicate a level in Be^8 , 2.05 MeV above the ground state. The experiment will be repeated in the near future.

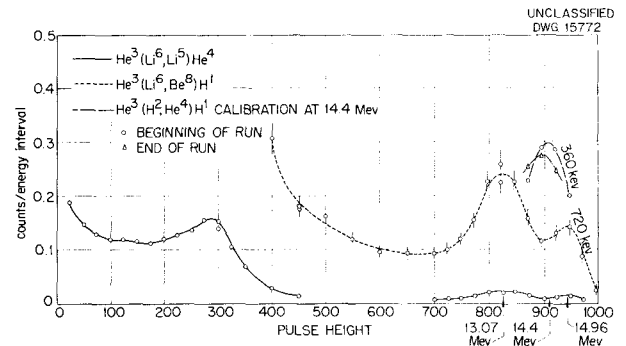


Fig. 1.3. Energy Spectrum of Particles from $\text{He}^3(\text{Li}^6, \text{Li}^5)\text{He}^4$ and $\text{He}^3(\text{Li}^6, \text{Be}^8)\text{H}^1$.

2. RADIOACTIVITY AND NUCLEAR ISOMERISM

ABSORPTION OF GAMMA RAYS

P. R. Bell J. E. Richardson
R. L. Heath

During the last quarter the scintillation spectrometer has been used to study the absorption of gamma rays. A thallium-activated sodium iodide crystal and the associated photomultiplier were placed inside a large, lead-walled shield, as shown in Fig. 2.1. The radiation source was suspended in air above the detector at point S. The absorber, in the form of large sheets, was placed across the top of the shield.

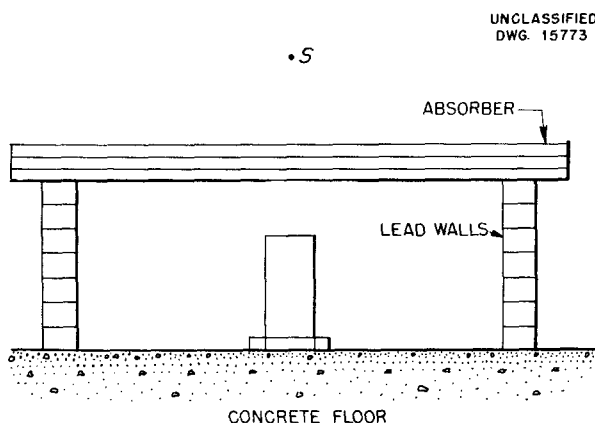


Fig. 2.1. Experimental Arrangement for Measuring Absorption Coefficients.

The photomultiplier was connected to a linear amplifier that in turn was connected to a 20-channel analyzer; thus it was possible to obtain the pulse spectrum produced by the radiation falling on the detector. This spectrum, in conjunction with the measured pulse spectrum from monoenergetic gamma rays, should permit a deduction of the gamma-ray spectrum of the radiation falling on the detector. This analysis has not yet been performed quantitatively and is not needed for the measurements of the absorption coefficients. The reason for this can best be seen by observing Fig. 2.2, which shows the pulse spectrum produced by Hg^{203} radiation with increasing thickness of aluminum absorber. The top curve was taken with no absorber and shows the typical photopeak from the 279-keV gamma ray and the associated Compton spectrum; the broad peak at

165 pulse-height divisions is due to back-scattering from the walls. If the curve taken through 4 in. of aluminum is considered, it is apparent that there is a considerable amount of degraded radiation owing to Compton scattering. There is also an appreciable amount of radiation at the full energy of 279 keV; just how much, can be determined by subtracting a fraction, f , of the original spectrum. The factor f is adjusted by repeated trials until the difference curve is quite smooth and shows no sign of a peak at the full energy. Thus, the amount of radiation arriving at the crystal that is unchanged in energy can be determined, that is, the fraction of the photons that go directly from source to detector without being scattered by either a photoelectric or a

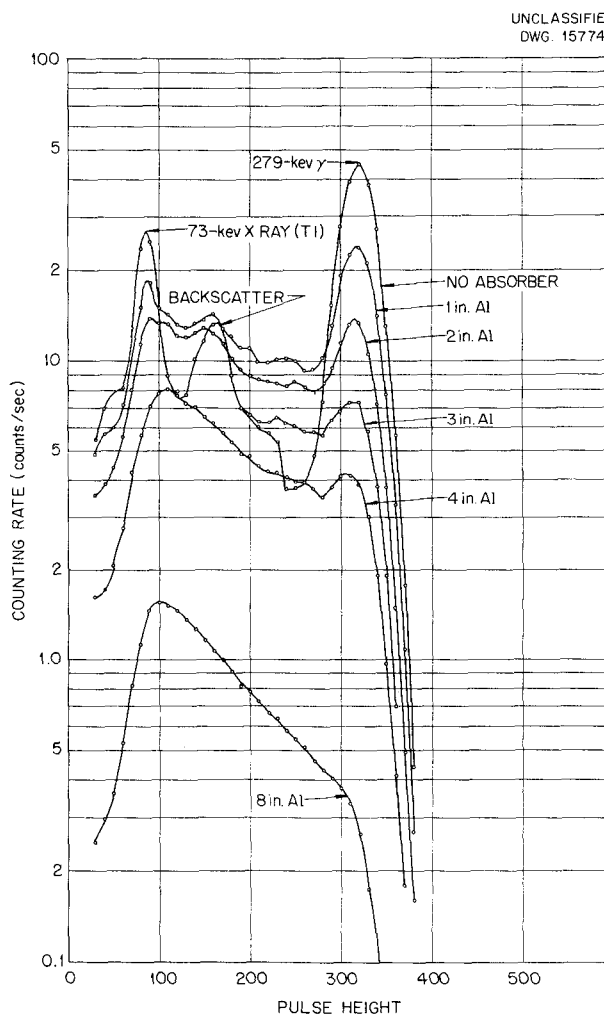


Fig. 2.2. Hg^{203} Gamma Absorption in Aluminum.

Compton process. The situation is somewhat complicated by coherent scattering that leaves the energy unchanged. Investigations are now being made to determine the amount and angular-dependence of coherent scattering. Figure 2.3 shows the absorption of gamma rays from Cs¹³⁷ in aluminum.

To date, the absorption of gamma rays in lead has been investigated more extensively than their absorption in aluminum. Sources of Hg²⁰³ (279 kev), Cs¹³⁷ (661 kev), Zn⁶⁵ (1.114 Mev), and Na²⁴ (2.76 Mev) have been used; the results are shown in Figs. 2.4, 2.5, 2.6, and 2.7. In contrast to the aluminum data, Fig. 2.4 shows that the radiation for the Hg²⁰³ source is not appreciably degraded in passing through 0.5 in. of lead, which indicates that photoelectric absorption is predominant. When a Na²⁴ source is employed, there is some buildup of lower energies, as can be seen from Fig. 2.4, but the buildup is much smaller than in aluminum.

A semilogarithmic plot of the intensity of the transmitted gamma ray, measured by the height of the photopeak vs. absorber thickness is shown in Fig. 2.8 for four different gamma-ray energies. The measured slope (multiplied by 2.30) is the absorption coefficient in factors of e per centimeter, as is indicated on each curve. By dividing by the density of lead ($\rho = 11.3$), the following values for the mass absorption coefficient are obtained:

GAMMA ENERGY	ABSORPTION COEFFICIENT (cm ² /g)
279 kev	0.465
661 kev	0.098
1.14 Mev	0.059
2.76 Mev	0.0412

The Bureau of Standards has measured the absorption coefficient of Cs¹³⁷ gamma rays in lead and has obtained a value of 0.106, which includes an estimated 0.005 for coherent scattering. This is in good agreement with measurements already obtained.

Determinations are being continued with higher gamma-ray energies and other absorbers. Of particular interest are the absorption measurements in sodium iodide. With these data it will be possible to calculate the absolute efficiencies of the scintillation detector.

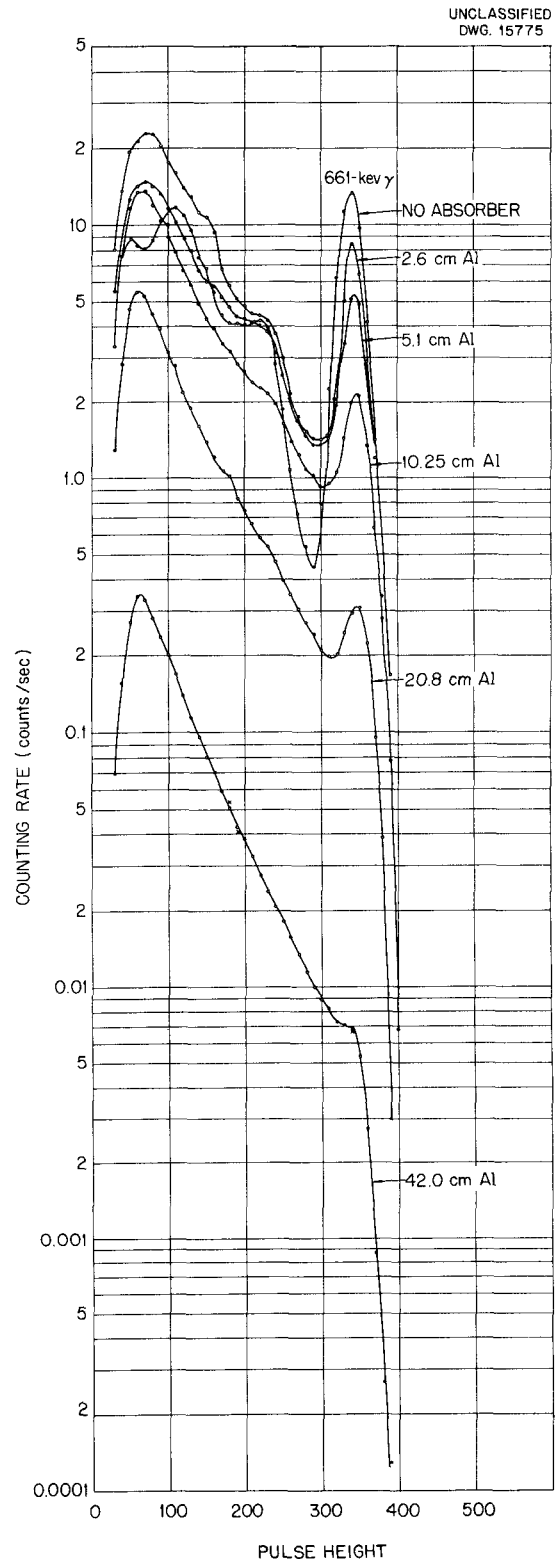


Fig. 2.3. Cs¹³⁷ Gamma Absorption in Aluminum.

RADIOACTIVITY AND NUCLEAR ISOMERISM

LIFETIME OF AN EXCITED STATE OF Hf¹⁷⁶

F. K. McGowan

An excited state in Hf¹⁷⁶ with a half life of $(1.35 \pm 0.10) \times 10^{-9}$ s has been observed with a delayed-coincidence scintillation spectrometer in which sources of Lu¹⁷⁶ (3.75 h) are used. The 89-keV isomeric transition is classified as E2 by

UNCLASSIFIED
DWG.15776

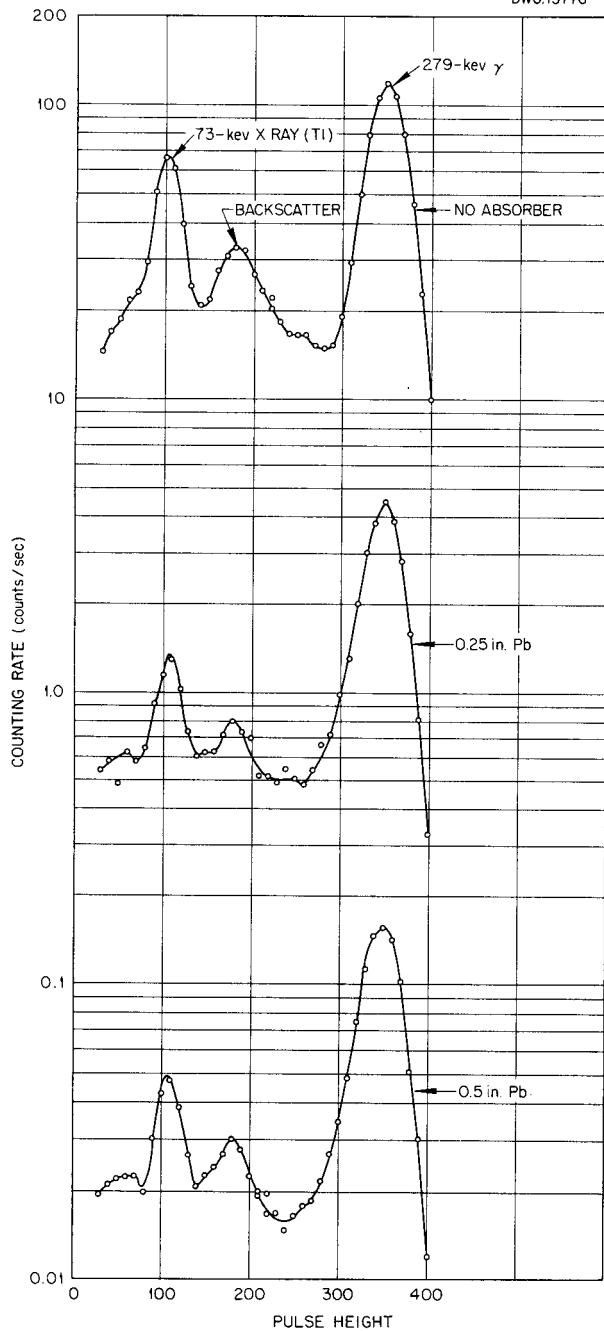


Fig. 2.4. Hg²⁰³ Gamma Absorption in Lead.

UNCLASSIFIED
DWG. 15777

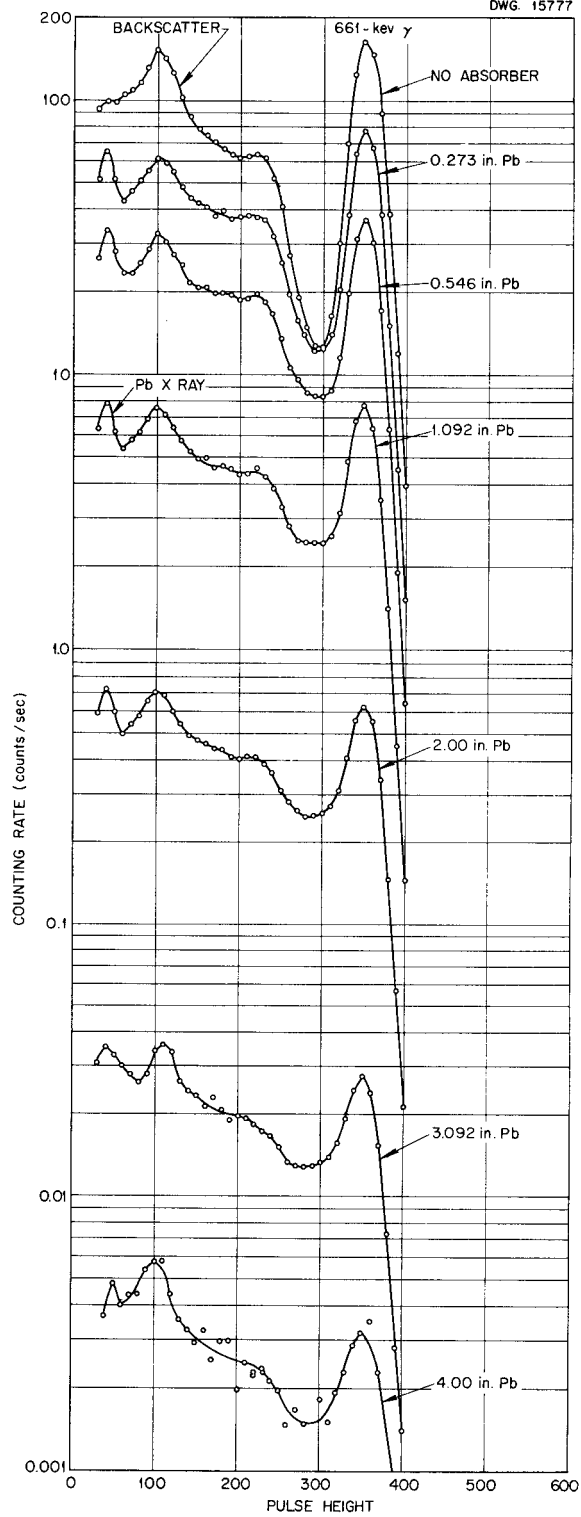


Fig. 2.5. Cs¹³⁷ Gamma Absorption in Lead.

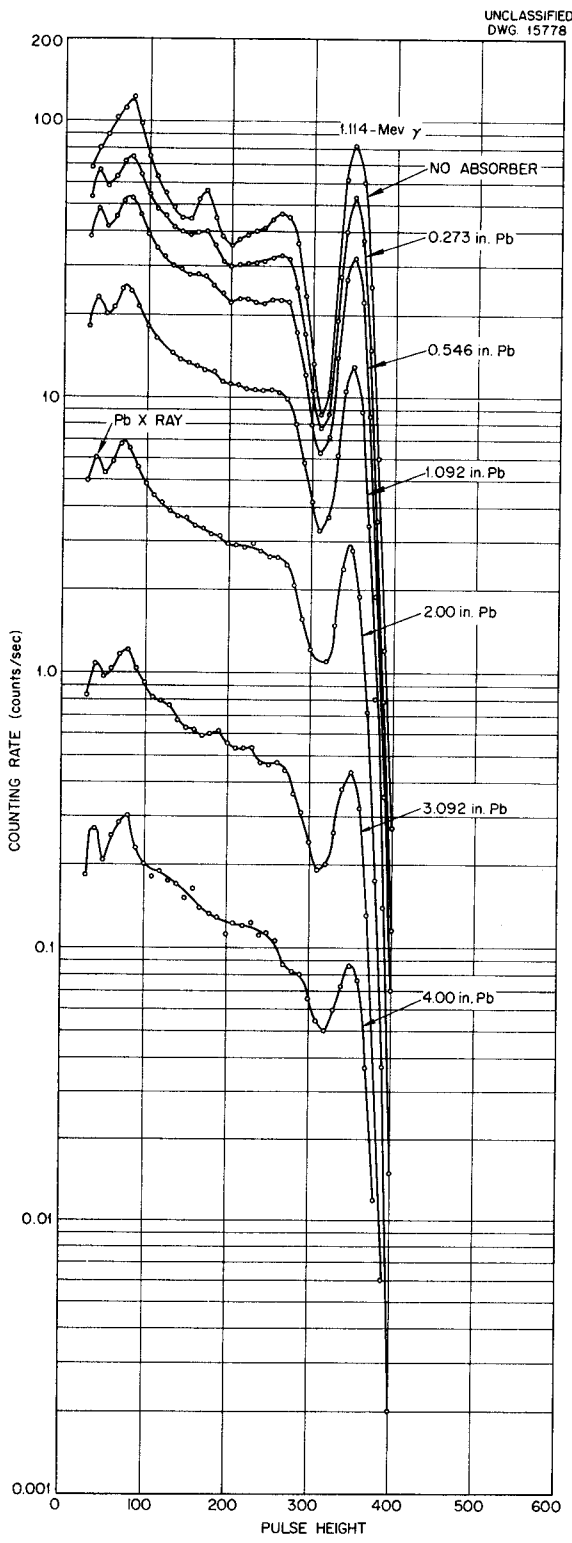


Fig. 2.6. Zn^{65} Gamma Absorption in Lead.

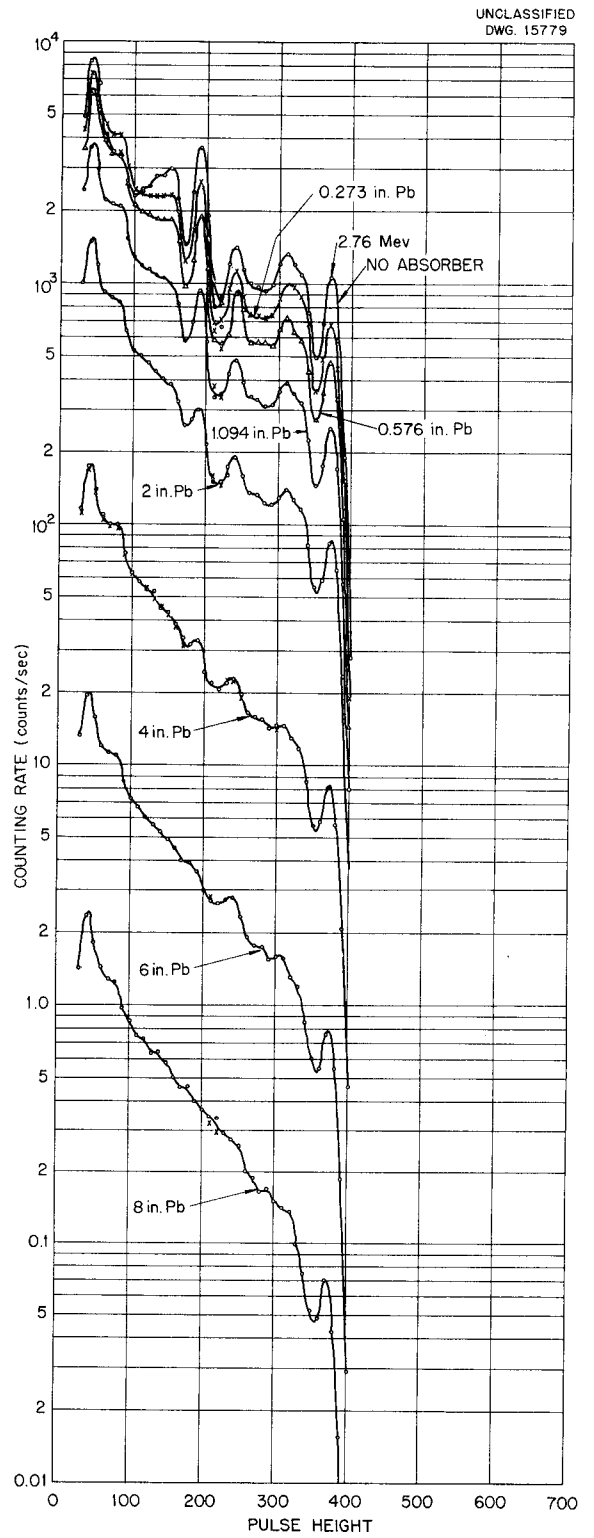


Fig. 2.7. Na^{24} Gamma Absorption in Lead. Measurements made with 1½-in.-dia by 1-in. thallium-activated sodium iodide crystal.

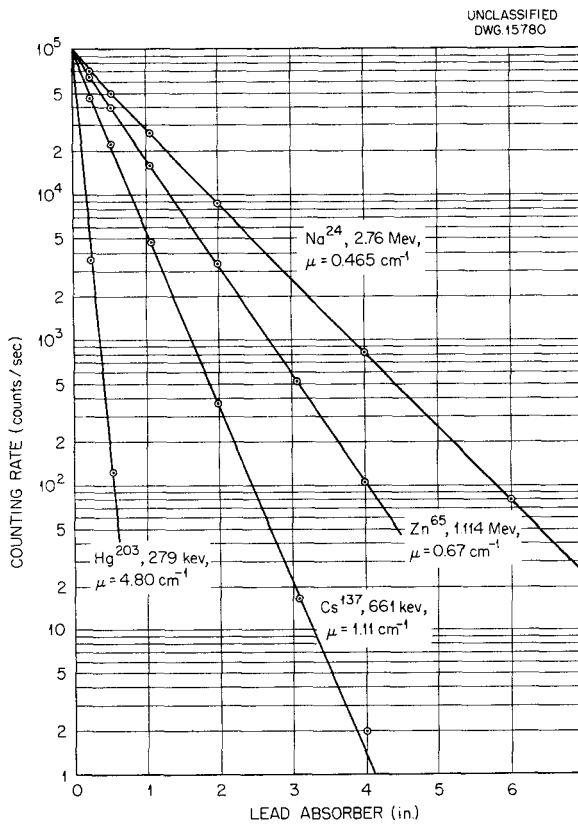


Fig. 2.8. Intensity of Photoelectric Peak as a Function of Absorber Thickness for Four Gamma-Ray Energies.

a measurement of the K-shell internal conversion coefficient. The results have been submitted for publication in *The Physical Review* as a "letter to the editor."

**GAMMA-GAMMA ANGULAR CORRELATION
IN Ta¹⁸¹**

F. K. McGowan

The intensities of the gamma-ray transitions following the β⁻ decay of Hf¹⁸¹ have been measured with a scintillation spectrometer employing sodium iodide detectors. The sources were prepared from a sample of HfO₂ enriched in Hf¹⁸⁰ (93.96%). The results of the measurements are shown in the decay scheme in Fig. 2.9.

The K-shell internal conversion coefficient of the 481-keV gamma-ray transition was obtained from intensity measurements of the K-shell internal conversion electrons and the gamma radiation with an anthracene and a sodium iodide scin-

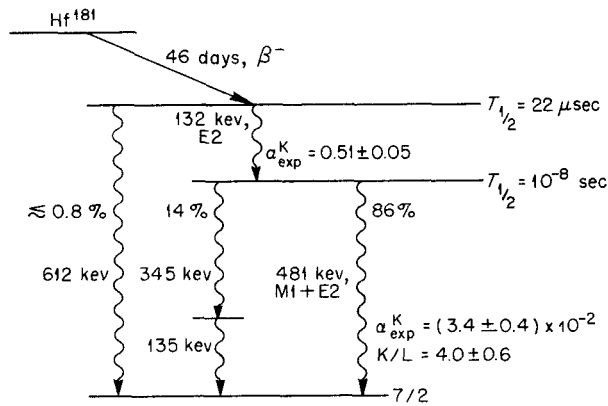


Fig. 2.9. Decay Scheme of Ta¹⁸¹.

tillation spectrometer, respectively. In one set of experiments the intensities were measured in coincidence with the 132-keV gamma radiation, and in another set of experiments the intensities were measured from the single-count spectrum. Good agreement was obtained between the two measurements. To check the method of measurement, the K-shell internal conversion coefficient of the 661-keV gamma-ray transition of Ba^{137*} was measured. The result agreed to within 6% of the accepted M4 assignment for the transition. In all experiments involving intensity measurements of the conversion electrons, the air between the source and the detector was displaced with hydrogen gas.

The experimental and theoretical internal conversion coefficients⁽¹⁾ are tabulated in the following list:

Nucleus	Ta ¹⁸¹
E _γ	481 keV
α ^K _{exp}	(3.4 ± 0.4) × 10 ⁻²

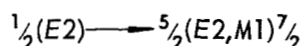
Theoretical Coefficients

a ^K ₁	0.64 × 10 ⁻²
a ^K ₂	1.74 × 10 ⁻²
a ^K ₃	4.40 × 10 ⁻²
β ^K ₁	6.00 × 10 ⁻²
β ^K ₂	16.4 × 10 ⁻²

(1) M. E. Rose, G. H. Goertzel, B. I. Spinrad, J. Harr, and P. Strong, *Phys. Rev.* 83, 79 (1951).

The 481-keV transition appears to be of the $M1 + E2$ type with a quadrupole-to-dipole intensity ratio of $1.6 + 0.7$ to $1.6 - 0.5$.

Because of the relatively large magnetic-dipole radiation intensity, which was not expected from the lifetime of the 481-keV transition, the gamma-gamma directional angular correlation of the 132-keV and the 481-keV cascades have been re-examined. The anisotropy for the sequence



is -0.62 for the conditions $\beta/\alpha = (1.6)^{1/2}$ and the electric and magnetic components out of phase in the Ling-Falkoff notation.⁽²⁾ A measured anisotropy of -0.15 for sources of HfO_2 dissolved in $\text{HF} + \text{HNO}_3$ was given in the last quarterly report.⁽³⁾

Since there may be an appreciable reorientation of the nuclear moment owing to the magnetic and electric fields of the electron shell during the lifetime of the intermediate state, the observed correlation may depend strongly on the medium in which the atom of the decaying nucleus is found. The normal-state configuration for tantalum is $5d^3 6s^2$; it exhibits a nonvanishing magnetic moment in the ground state of the free atom. Thus, it appears desirable to have the tantalum atom highly ionized (Ta^{5+}). To test this point, several ionic solutions of the radioactive material have been prepared. An appreciable effect of the chemical state of the Hf^{181} sources on the angular correlation has been observed. Preliminary results are shown in Table 2.1.

⁽²⁾D. S. Ling, Jr. and D. L. Falkoff, *Phys. Rev.* 76, 1639 (1949).

⁽³⁾F. K. McGowan, *Physics Division Quarterly Progress Report for Period Ending March 20, 1952*, ORNL-1289, p. 10.

ANGULAR CORRELATION OF GAMMA RAYS

E. D. Klema F. K. McGowan

The measurement of the angular correlation of the gamma rays emitted in the decay of excited states of Cd^{114} has been completed. The correlation obtained,

$$\omega(\theta) = 1 + 0.111 P_2(\cos \theta) + 0.023 P_4(\cos \theta)$$

or

$$\omega(\theta) = 1 + 0.084 \cos^2 \theta + 0.106 \cos^4 \theta,$$

makes possible the spin assignment of 0-2-2 for the ground state and the two excited states of Cd^{114} , respectively. The first gamma ray of the cascade is a mixture of 97% magnetic dipole and 3% electric quadrupole radiation, with the electric and magnetic components in phase. These results have been submitted to *The Physical Review* for publication.

SHORT-PERIOD ACTIVITIES

E. C. Campbell

Germanium. A new isomer of short half life has been found in each of several samples of germanium irradiated in the fast pneumatic tube with reactor neutrons. A preliminary measurement of the half life (by the method described in the material following) gives 0.35 second. This result is only approximate, since the decay could be followed through only about two half lives owing to the presence of another activity of longer half life. This activity is presumably to be identified with the 42-s isomer found by Flammersfeld,⁽⁴⁾ who determined that conversion electrons with an

⁽⁴⁾A. Flammersfeld, *Z. Naturforsch.* 7a, 296 (1952).

TABLE 2.1. EFFECT OF CHEMICAL STATE ON ANGULAR CORRELATION

SAMPLE	FORM	ANISOTROPY
$\text{Hf}(\text{OH})_4$	Dry	-0.086
$\text{Hf}(\text{OH})_4$	0.025 ml of solution	-0.098
HfO_2	Dissolved in 0.020 ml of HF and HNO_3	-0.19
HfO_2	Dissolved in 0.15 ml of HF	-0.33
HfO_2	Dissolved in 0.50 ml of HF	-0.34
Hf	Hafnium metal	-0.07

LOW-TEMPERATURE PHYSICS

energy of 140 keV were associated with it. If these are K conversion electrons, the transition energy is 151 keV.

Pulses from a sodium iodide scintillation detector that were observed on the screen of a cathode-ray oscilloscope showed the existence of two gamma rays, one associated with each of the two periods. The pulses that are associated with the 0.35-s period are seen only very briefly and have somewhat less than half the amplitude of those associated with the longer period. If the latter pulses are identified with the 151-keV gamma ray expected from the 42-s isomer, the energy of the 0.35-s gamma must be approximately 60 keV. The half life and the energy values are preliminary estimates.

Ytterbium. The half life of the isomer in ytterbium previously estimated⁽⁵⁾ as less than 0.5 s has been measured. The method used consists

of recording scaler output pulses on rapidly moving paper with a crystal-controlled pen. The speed of the paper is monitored during the decay by another scaler running on the line frequency, the output of which actuates a second similar pen writing on the same paper. The value obtained was 0.15 ± 0.05 second. This is the shortest half life of any isomer found with the present equipment.

Lead. The half life of the short-period isomer in lead previously reported as 0.9 s has been measured by the method described in the preceding paragraph. The result is 0.84 ± 0.03 s, which is in agreement with the value 0.82 ± 0.02 s obtained by Lascoux and Vendryes.⁽⁶⁾

(5) J. H. Kahn, *An Investigation of X-Ray and Gamma Ray Spectra of Short Period Radioisotopes*, ORNL-1089, (Oct. 24, 1951).

(6) J. Lascoux and G. Vendryes, *Compt. Rend.* 233, 858 (1951).

3. LOW-TEMPERATURE PHYSICS

ELECTRICAL RESISTANCE OF HIGH-PURITY ZIRCONIUM BELOW 300°K

L. D. Roberts C. C. Sartain⁽¹⁾
J. W. T. Dabbs

If a crystal were composed of many identical metallic atoms arrayed in a perfect lattice it would have no electrical resistance.⁽²⁾ If the lattice is not perfectly periodic, however, the resulting scattering of electrons will give rise to resistance. Departure from perfect periodicity may be due to the displacement of atoms from their mean position owing to thermal motion or to the presence of foreign atoms. A third departure may be the breakdown of the lattice itself, for example, into a polycrystal. By assuming that the electrons in a metal are free, Bloch⁽³⁾ and Grüneisen⁽⁴⁾ have developed a formula for the resistance of a pure

metal caused by the thermal displacement of the atoms.

$$R \propto \left(\frac{T}{\theta}\right)^5 \int_0^{\theta/T} \frac{x^5 dx}{(e^x - 1)(1 - e^{-x})} = TG(x), \quad (1)$$

where θ is the Debye temperature. For $T \ll \theta$, they obtained $R \propto T^5$; for large values of T , $R \propto T$, since for this case the integral approaches $(1/4)(\theta/T)^4$.

Baber,⁽⁵⁾ by taking into account the collision of electrons with positive holes, has found an additional term, $R \propto T^2$. De Haas and de Boer⁽⁶⁾ have found that for nickel, palladium, and platinum,

$$R = KT^2 + R_G, \quad (2)$$

where R_G is the resistance given by the Grüneisen formula, Eq. 1. They found that for platinum the KT^2 term is dominating below 10°K.

(1) Research participant from the University of Alabama.

(2) N. F. Mott and H. Jones, *Theory of the Properties of Metals and Alloys*, p. 243, The Clarendon Press, Oxford, 1936.

(3) F. Bloch, *Z. Physik* 52, 555 (1929); F. Bloch, *Z. Physik* 59, 208 (1930).

(4) E. Grüneisen, *Ann. Physik* 16, 530 (1933).

(5) W. G. Baber, *Proc. Roy. Soc. (London)* A158, 383 (1937).

(6) W. J. de Haas and J. de Boer, *Physica* 1, 609 (1934).

Houston⁽⁷⁾ reports that when T/θ is not too large, the resistance will vary with a lower power of T than T^5 , and only for extremely low values of T will the fifth-power dependence be reached. Measurements on sodium made by MacDonald and Mendelssohn⁽⁸⁾ confirm this.

Adenstedt⁽⁹⁾ has found that for high-purity zirconium between 300 and 1300°K, $R \propto T^n$, where n is slightly less than one. No measurements on high-purity samples of this metal at low temperatures have been reported.

Three samples of high-purity crystal-bar zirconium have been secured and the resistivity of sample 1, unannealed, was measured at three temperatures (see Table 3.1). The values agree with those obtained by Adenstedt at 0°C.

TABLE 3.1. RESISTIVITY OF HIGH-PURITY CRYSTAL-BAR ZIRCONIUM, SAMPLE 1, UNANNEALED

T (°K)	ρ ($\mu\text{ohm-cm}$)
295.7	45.6
73.3	8.68
4.2	2.14

Sample 1 was subsequently pickled in an aqueous solution of nitric and hydrofluoric acids and then was annealed in a vacuum for 40 min at $796 \pm 14^\circ\text{C}$. The ± 14 deg was due to known thermal gradients in the furnace and not to a variation in the temperature with time. The sample was cooled in air and repickled. Since pickling removed some material, absolute resistivity can be computed only after the sample dimensions are remeasured. The resistance of sample 1, after annealing, has been measured for a number of temperatures, including ambient temperatures and those of melting ice and of liquid nitrogen and hydrogen at various pressures. The ratio of the resistance, R , as a function of temperature to the value of R at 0°C is given in Table 3.2.

If Matthiessen's rule that a small amount of impurity in a solid solution produces a resistance

(7)W. V. Houston, *Proceedings of the International Conference on Low Temperature Physics*, p. 45, Oxford, August 22 to 28, 1951.

(8)D. K. C. MacDonald and K. Mendelssohn, *Proc. Roy. Soc. (London)* A202, 103 (1950).

(9)H. K. Adenstedt, Paper No. 1 W, American Society of Metals Midwinter Meeting, Pittsburgh, January 31 to February 1, 1952.

that is independent of temperature is accepted and if the T^2 term that represents electron-hole collisions is neglected, a first approximation is obtained at low temperatures in which

$$R = A + BT^5. \quad (3)$$

Upon fitting this equation to the measured values of resistance at 20.33 and 14.01°K, it is found that

$$A = 4.135 \times 10^{-3} \text{ ohms}$$

and

$$B = 1.484 \times 10^{-10} \text{ ohms/deg}^5.$$

A comparison of $R - A$ with BT^5 and with $B_1T^{4.5}$ is given in Tables 3.3 and 3.4. It is seen from this comparison that between 14 and 20°K, the resistance of sample 1 appears to follow a T^n law, but with n less than 4.5 instead of 5. It cannot now be stated whether this behavior is due to a less-than- T^5 law as suggested by Houston, or perhaps to a term proportional to T^2 added to the T^5 law as suggested by Baber. Measurements on sample 1 will be extended to the liquid-helium temperature range, and its absolute resistivity will be determined. Samples 2 and 3 are being prepared for measurement. It is hoped that these proposed measurements will decide which law is followed by actual samples.

MacDonald⁽¹⁰⁾ has developed a technique for

(10)D. K. C. MacDonald, private communication.

TABLE 3.2. RATIO OF RESISTANCE AT VARIOUS TEMPERATURES TO RESISTANCE AT 0°C* FOR SAMPLE 1

T (°K)	R/R_0
300.3	1.1245
273.2	1.0000
77.50	0.17356
68.52	0.14076
20.33	0.02514
14.01	0.02279

*Temperature coefficient of resistance at 273.2°K, $\alpha_0 = 4.59 \times 10^{-3}/\text{deg}$.

LOW-TEMPERATURE PHYSICS

TABLE 3.3. COMPARISON OF RESIDUAL RESISTANCE WITH THE FIFTH-POWER LAW

$$R = 4.135 \times 10^{-3} + 1.484 \times 10^{-10} T^5$$

T (°K)	T^5 (deg ⁵)	BT^5 (ohms)	$R - A$ (ohms)
20.33	34.73×10^5	51.54×10^{-5}	51.54×10^{-5}
18.91	24.18×10^5	35.88×10^{-5}	37.25×10^{-5}
17.13	14.75×10^5	21.89×10^{-5}	23.77×10^{-5}
14.01	5.397×10^5	8.010×10^{-5}	8.011×10^{-5}

TABLE 3.4. COMPARISON OF RESIDUAL RESISTANCE WITH A LESS-THAN-FIFTH-POWER LAW

$$R = 4.115 \times 10^{-3} + 6.953 \times 10^{-10} T^{4.5}$$

T (°K)	$T^{4.5}$ (deg ^{4.5})	$B_1 T^{4.5}$ (ohms)	$R - A_1$ (ohms)
20.33	7.703×10^5	5.355×10^{-4}	5.355×10^{-4}
18.91	5.560×10^5	3.866×10^{-4}	3.926×10^{-4}
17.13	3.564×10^5	2.478×10^{-4}	2.578×10^{-4}
14.01	1.442×10^5	1.002×10^{-4}	1.002×10^{-4}

calculating the Debye θ from resistance measurements based on the ratio,

$$\frac{\frac{dR}{dT}}{\frac{R}{T}} = 1 + x \frac{\left| \frac{dG}{dx} \right|}{G}, \quad (4)$$

where $x = \theta/T$, and G is the Grüneisen function (Eq. 1). By using this technique it is necessary to know only the resistance and its slope at a given temperature to obtain a θ value. The assumptions involved, if the derived θ is to be truly characteristic of the lattice, are: (1) that the resistance must be essentially thermal in origin, which means that, in particular, the residual resistance should always be subtracted, but this is not important at moderate temperatures in a pure metal; (2) that the Bloch-Grüneisen formula is accepted as a sufficiently adequate approximation for the ideal resistance of a metal; and (3) that θ is not varying rapidly ($d\theta/dT \ll \theta/T$), otherwise a correction should be strictly applied for a term involving $d\theta/dT$. However, the estimate of θ in this respect should be just as valid as that from a

Debye formula in calorimetric work. The term on the left of Eq. 4 has been determined from experiment at 273, 77, and 20°K. The corresponding values of θ are 281, 239, and 146 degrees. Since the value of θ obtained in this way is not constant, whereas the technique of calculation assumes a constant θ , it must be concluded that these θ values are only approximate. However, the value of 281 deg at $T \simeq \theta$ agrees well with the value of 288 deg computed from measurements made by Grüneisen.⁽⁴⁾

PARAMAGNETISM OF TRIVALENT URANIUM

L. D. Roberts J. W. T. Dabbs
C. C. Sartain

The investigation of the spin-dependence of neutron capture by U^{235} and U^{233} , and thus the alignment of these nuclei, is an experiment of some importance. The alignment can, in principle, be effected by either of two techniques: the direct alignment of the nucleus by the application of a very large magnetic field (of the order of 100,000 gauss) at some very low temperature (of the order

of 0.01°K), or through the use of hyperfine-structure coupling. Since the latter procedure is in many respects the simpler of the two, it was desirable to find a compound of uranium that was paramagnetic at liquid-helium temperatures and below and then to determine the magnitude of the hyperfine-structure coupling by measuring the specific heat of this compound near 1°K for several different uranium isotopes.

Previous studies of the paramagnetism of the uranium compounds have been made principally on the tetravalent state. These compounds have a very large Weiss constant in the region of 40 to 180°K and thus do not display any temperature-dependent magnetic effects in the vicinity of 1°K .

Recent studies of the magnetism of trivalent uranium halides by Dawson⁽¹¹⁾ have shown that they become antiferromagnetic at approximately 300°K , and thus the pure trivalent halides are also unsuitable.

When a molecule that is paramagnetic in the free state is subjected to an electric field, the angular-momentum degeneracy will in general be lifted to some degree, depending on the symmetry of the electric field. According to a theorem by Kramers, however, if the molecule has an odd number of magnetic electrons, the ground state will remain at least doubly degenerate and the molecule will have a paramagnetism corresponding to this degeneracy. The trivalent uranium halide molecules have an odd number of electrons and thus should be paramagnetic at temperatures near 1°K if it were not for the fact that spin-exchange coupling leads to antiferromagnetism, as was just indicated. These facts suggested that a dilute solid solution of a trivalent uranium halide in

some isomorphous nonmagnetic material should be paramagnetic at low temperatures.

According to the x-ray measurements made by Zachariasen,⁽¹²⁾ uranium trifluoride and lanthanum trichloride are isomorphous to better than 1% and thus should be suitable components for the solid solution mentioned in the preceding paragraph. However, the preparation of a solid solution between the lanthanum halides and the uranium halides presents some difficulties of a chemical nature. At temperatures of the order of 900 to 1000°C the uranium halides tend to disproportionate. It was for this reason that uranium trifluoride, which is the most stable of the uranium compounds toward disproportionation, was dissolved in lanthanum trichloride, which has a somewhat lower melting point, 860°C . The fusion is performed in dry hydrogen to keep the uranium in the trivalent state.

A solid solution containing 10 mole % of uranium trifluoride and lanthanum trichloride has been prepared by D. E. LaValle of this laboratory, and a powder sample has been found to be paramagnetic in the temperature region between 1 and 4°K and to have a Curie constant approximately of the magnitude to be expected for a Kramers degeneracy. Recent measurements by Ghosh, Gordy, and Hill⁽¹³⁾ indicate a g factor for trivalent uranium of about 2.4. With a g factor deviating so far from 2 it is unlikely that the susceptibility would be isotropic, and thus it is not permissible to calculate a Curie constant from the preceding measurements on a powder sample. These measurements on trivalent uranium solid solutions are being continued.

(11) J. K. Dawson, *The Magnetic Susceptibilities and Electronic Structures of the Halides of Ter- and Quadrivalent Uranium*, AERE-C/R-578, Harwell (Sept. 1950).

(12) W. H. Zachariasen, *Acta Cryst.* 1, 265 (1948).

(13) S. N. Ghosh, W. Gordy, and D. G. Hill, *Phys. Rev.* 87, 229 (1952).

4. HEAVY-ION PHYSICS

AVERAGE ENERGY PER ION PAIR

G. E. Evans P. M. Stier
C. F. Barnett

The major effort of the heavy-ion physics group during the last quarter has been devoted to a study of different techniques suitable for the routine measurement of W , the electron volts per ion pair. A number of preliminary experiments have been carried out by using the differential-pumping entrance-pinhole system, described previously,⁽¹⁾ that employed ions of varying mass and energy which were produced in the Cockcroft-Walton accelerator.

An initial attempt was made to measure the total ionization produced by the beam by stopping the beam in an ion chamber that was large compared to the range. To reduce ion-collection distances and to improve potential gradients, the ion chamber was constructed to include three collecting wires and three ground wires, which were distributed parallel to each other and the beam in hexagonal symmetry. It was not found possible to saturate the ion chamber owing to low collecting efficiency in several of the stopping gases employed. The direct beam current was measured by using a small Faraday cup mounted on a rod sliding in a Wilson seal so that the Faraday cup could be moved to intercept the beam at a point about $\frac{1}{8}$ in. below the entrance pinhole. Attempts to read the beam current with gas in the scattering chamber were unsuccessful, since under these circumstances the Faraday cup acts as an ion chamber, with ion currents larger than the direct beam current. It was found possible to measure the positive-ion beam by reading the Faraday-cup current at saturation for both positive- and negative-ground ring bias, since the direct positive-ion current is equal to half the algebraic sum of the two saturation currents. However, this technique involves the measurement of a small difference of large quantities and was discarded because of the low accuracy it permitted.

Experiments were carried out to determine the feasibility of monitoring the direct beam by the luminescence produced in various materials. To

eliminate the high background produced in the photomultiplier tube by gas luminescence, differences in light emission between two different target materials were measured at different beam energies and intensities. The most satisfactory pair of materials studied was quartz and mica. The calibration of the monitor changed fairly rapidly with bombardment time as a result of darkening of the crystal surfaces, and the experiments were discontinued. It is planned to continue the study of light emission from targets bombarded by low-energy positive ions under more favorable experimental conditions (by using low beam intensities and high vacuum).

The method finally used for the measurement of W is as follows: A suitable steady-state gas pressure of several millimeters of mercury is established in a large gas chamber attached to the entrance pinhole and differential pumping system. The ionization produced by a collimated beam of heavy ions passing through the pinhole system is measured with a thin (0.130 in.) parallel-plate ion chamber 7 in. in diameter and constructed with high-transparency fine-wire grids. The chamber is normally operated with the collector plate at ground potential and the wire grid at about 45 v negative. The upper surface of the ion chamber is shielded with a second wire grid attached to ground. The ion chamber is attached to a rod that is parallel to the beam axis and which can be raised and lowered to measure the ionization density as a function of range (distance from the entrance pinhole). The total number of ions produced per second in the gas volume is determined by integrating the ionization current over the entire range. The gas chamber is then evacuated to a pressure sufficiently low for gas ionization effects to be ignored ($<10^{-4}$ mm Hg), whereas the beam energy and intensity are allowed to remain constant. Since this evacuation also lowers the pressures in the differential pumping system, gas is allowed to leak into the region between the differential pumping pinholes to keep the effective window thickness constant. The positive ion beam is then read by using a Faraday cup mounted so as to permit its withdrawal from the gas chamber during the initial portion of the experiment.

The largest probable error in this technique arises from possible shifts in beam intensity

(1) G. E. Evans, C. F. Barnett, P. M. Stier, and V. L. DiRito, *Physics Division Quarterly Progress Report for Period Ending December 20, 1951*, ORNL-1278, p. 17.

during the time required to pump down the gas volume (about 2 min). The maximum deviations from the mean on repeat runs have been less than 10% and the bulk of the data is self-consistent to within 2%.

The actual values of W depend linearly upon the effective thickness of the ion chamber, which has

not yet been measured. Upon completion of the present survey of W in various gases and at various energies, the geometrical thickness of the chamber will be readjusted. The effective thickness can then be determined from the variation in response as a function of geometrical thickness.

5. NEUTRON CROSS SECTIONS

NEUTRON CROSS-SECTION MEASUREMENTS FOR POLYCRYSTALLINE NICKEL AND NICKEL OXIDE IN THE THERMAL ENERGY REGION

R. G. Allen

A simple method for extending the useful range of a neutron crystal spectrometer to wave lengths as long as 4 or 5 Å has been described in a previous quarterly report.⁽¹⁾ This method makes use of the total reflection and selective attenuation properties of mirrors for neutrons incident at small glancing angles in order to remove the higher order reflections from the crystal. This apparatus was first used for cross-section measurements of the relatively large absorbers, gold, indium, and silver; these results are reported in the previous quarterly report.⁽¹⁾

For many substances, the crystalline scattering effects are most prominent in the wave-length region between 1 and 5 Å, and appear as discontinuities in the total cross section as a function of wave length at those wave lengths satisfying the relation,

$$\lambda = 2d_{h_1 h_2 h_3} \quad (1)$$

where λ is the neutron wave length and $d_{h_1 h_2 h_3}$ is the plane spacing for the plane described by the Miller indices $h_1 h_2 h_3$. In the case of a monatomic crystal, a measurement of the height of a single discontinuity is sufficient to determine the nuclear coherent-scattering amplitude, provided the Debye characteristic temperature is known. However, if the heights of several discontinuities are measured, it is possible to determine the Debye temperature as well as the coherent-scattering amplitude. Finally, if measurements are made over a wide wave-length region, from wave lengths longer than

⁽¹⁾R. G. Allen, T. E. Stephenson, and T. I. Arnette, *Physics Division Quarterly Progress Report for Period Ending September 20, 1951*, ORNL-1164, p. 38.

the Bragg cutoff to wave lengths sufficiently short for the crystalline scattering effects to be small, it is possible to obtain information concerning the total-scattering cross section, the incoherent-scattering cross section, and the inelastic-scattering cross section, as well as the Debye temperature and the coherent-scattering cross section previously mentioned.

The total cross section was measured by a transmission method using the customary relation

$$\sigma_t = \frac{1}{Nt} \ln T \quad (2)$$

where σ_t is the total measured cross section, N is the number of nuclei per cubic centimeter, t is the sample thickness, and T is the transmission of the sample defined by

$$T = \frac{I_1 - I_3}{I_0 - I_2} \quad (3)$$

in which I_0 , I_1 , I_2 , and I_3 are the measured intensities of the incident beam, the transmitted beam, the incident beam background, and the transmitted beam background, respectively.

The total cross section, being a measure of the loss of neutrons from the beam as a result of all causes, may be represented by the expression

$$\sigma_t = \sigma_{\text{capture}} + \sigma_{\text{scattering}} \quad (4)$$

The capture cross section (σ_{capture}) may be taken as proportional to the wave length in the wave-length region of these measurements, and the scattering cross section may be represented by

$$\sigma_{\text{scattering}} = \sigma_{\text{incoherent}} + \sigma_{\text{coherent}} + \sigma_{\text{inelastic}} + \sigma_{\text{magnetic}} \quad (5)$$

NEUTRON CROSS SECTIONS

The incoherent cross section arises from the presence of isotopes and nuclear spins; the coherent cross section gives the contribution to the scattering that results from interference effects because of the crystalline nature of the material; the inelastic term results from interchanges of energy between the incident neutrons and the crystal lattice; and the magnetic cross section describes the scattering that results from the interaction between neutrons and the magnetic moment of the atom. For the crystalline state, the magnetic scattering is generally quite small compared with the nuclear scattering, but it can become appreciable for some materials.^(2,3)

The results of the theoretical investigations of the scattering of slow neutrons by polycrystalline materials by Halpern, Hamermesh, and Johnson,⁽⁴⁾ Weinstock,⁽⁵⁾ Cassels,⁽⁶⁾ and Kleinman⁽⁷⁾ give the following expression for the scattering cross section:

$$\begin{aligned} \sigma_{\text{scattering}} = & \sigma_{\text{incoherent elastic}} \\ & + \sigma_{\text{coherent elastic}} + \sigma_{\text{incoherent inelastic}}^{+1} \\ & + \sigma_{\text{incoherent inelastic}}^{-1} + \sigma_{\text{coherent inelastic}}^{+1} \\ & + \sigma_{\text{coherent inelastic}}^{-1} \end{aligned} \quad (6)$$

$$\frac{\sigma_{\text{coherent elastic}}}{\text{nucleus}} = \frac{\sigma_{\text{coherent}} N \lambda^2}{8\pi} \sum_{\lambda < 2d_{h_1 h_2 h_3}}$$

(2) C. G. Shull and J. S. Smart, *Phys. Rev.* **76**, 1256 (1949).

(3) C. G. Shull, W. A. Strauser, and E. O. Wollan, *Phys. Rev.* **83**, 333 (1951).

(4) O. Halpern, M. Hamermesh, and M. H. Johnson, *Phys. Rev.* **59**, 981 (1941).

(5) R. Weinstock, *Phys. Rev.* **65**, 1 (1944).

(6) J. M. Cassels, "The Scattering of Neutrons by Crystals," *Progress in Nuclear Physics*, Vol. 1, p. 185, Academic Press, New York, 1950.

(7) D. A. Kleinman, Dissertation, Brown University, August 1951.

where

$$\frac{\sigma_{\text{incoherent elastic}}}{\text{nucleus}} = \sigma_{\text{incoherent}} \left\{ \frac{\lambda^2}{P} (1 - e^{-P/\lambda^2}) \right\} \quad (7)$$

$$P = \frac{12h^2}{Mk_0 T} \Phi(x),$$

$$\Phi(x) = \frac{1}{x} \left\{ \frac{\phi(x)}{x} + \frac{1}{4} \right\},$$

$$\phi(x) = \frac{1}{x} \int_0^x \frac{\beta d\beta}{e^\beta - 1},$$

$$x = \frac{\theta}{T},$$

in which

h = Planck's constant,

M = mass of atom,

k_0 = Boltzmann constant,

T = temperature of material ($^{\circ}\text{K}$),

θ = Debye characteristic temperature,

λ = neutron wave length (\AA).

$$J_{h_1 h_2 h_3} d_{h_1 h_2 h_3} |F_1|^2 e^{-2M_{h_1 h_2 h_3}}, \quad (8)$$

where

N = number of nuclei per cubic centimeter of crystal,

$J_{h_1 h_2 h_3}$ = multiplicity associated with the planes given by the Miller indices $h_1 h_2 h_3$,

$d_{h_1 h_2 h_3}$ = $h_1 h_2 h_3$ plane spacing.

The crystal-structure factor per nucleus (F_1) is given by

$$F_1 = \frac{1}{n} \sum_{\substack{i \\ \text{unit cell}}} \bar{f}_{\text{coherent}} e^{2\pi i[x_j h_1 + y_j h_2 + z_j h_3]}, \quad (9)$$

where n is the number of nuclei per unit cell, x_j , y_j , and z_j are the coordinates of the j th nucleus in the unit cell in units of the lattice constants, $\bar{f}_{\text{coherent}}$ is the average coherent scattering amplitude for the type of nucleus at the j th site, and $M_{h_1 h_2 h_3}$ is the Debye-Waller exponent resulting from the thermal motions of the atoms of the lattice.

$$2M_{h_1 h_2 h_3} = \frac{1}{4} \frac{P}{d_{h_1 h_2 h_3}^2}, \quad (10)$$

P being given in Eq. 7.

Expressions for each of the inelastic cross sections given in Eq. 6 can be obtained from the work of Weinstock⁽⁵⁾ and Cassels.⁽⁶⁾ These cross

$$\sigma_{\text{scattering}} = \sigma_{\text{incoherent}} + \sigma_{\text{coherent}} \left[1 - \frac{\lambda^2}{p} (1 - e^{p/\lambda^2}) \right] + \sigma_{\text{coherent elastic}}, \quad (12)$$

sections, however, represent the inelastic scattering in which only a single phonon of energy is exchanged between a neutron and the crystal lattice and are not valid at higher energies. The (-1) signifies absorption of one phonon by the neutron, i.e., the quenching of one of the vibrational modes of the lattice, whereas $(+1)$ signifies the emission of one phonon by the neutron or the excitation of a lattice mode. Calculations of the cross sections by using these formulas are tedious. Kleinman,⁽⁷⁾ however, presents a relatively simple method for calculating the total inelastic-scattering cross sections for one phonon process based on what he calls the "incoherent approximation." This expression is of the form

$$\sigma_{\text{inelastic}}^{\pm 1} = \left\{ \sigma_{\text{coherent}} + \sigma_{\text{incoherent}} \right\} \frac{m E}{M \theta} I \left(\frac{E}{\theta}, \frac{T}{\theta} \right), \quad (11)$$

where

$$I = F \left(\frac{E}{\theta}, \frac{T}{\theta} \right) - r f(r) G \left(\frac{E}{\theta}, \frac{T}{\theta} \right),$$

m = neutron mass,

M = mass of scattering nucleus,

E = energy of neutron expressed as a temperature ($^{\circ}\text{K}$),

θ = Debye characteristic temperature,

T = temperature of scatterer ($^{\circ}\text{K}$),

$r = 6 \frac{m E}{M \theta} \left\{ \frac{\phi(x)}{x} + \frac{1}{4} \right\}$, where $\left\{ \frac{\phi(x)}{x} + \frac{1}{4} \right\}$ is given in Eq. 7.

F , G , and $f(r)$ are functions that Kleinman has evaluated numerically in his paper.⁽⁷⁾

If a scattering model is assumed in which the atoms execute independent thermal oscillations with the same average energy, an expression for the total scattering cross section may be obtained in a manner similar to that used in obtaining the x-ray diffuse scattering.⁽⁸⁾ This approximation, although admittedly crude, apparently gives results that agree with the measured results of this work fairly well at intermediate and short wave lengths. The total scattering cross section from this "independent oscillator" approximation is

where the symbols have the same meaning as in Eqs. 7 and 8. This expression predicts a type of conservation of scattering, that is, the scattering lost in the coherent elastic scattering appears in the thermal diffuse scattering; the second term on the right of Eq. 12 is called the thermal diffuse-scattering cross section.⁽⁹⁾

If the scattering substance contains more than one species of atom, the formulas must be slightly modified to account for the different types of scattering atoms. This may be done for the coherent elastic cross section by using the average atomic mass in the Debye-Waller exponent and by including the coherent scattering amplitudes in the structure

⁽⁸⁾R. W. James, *The Optical Principles of the Diffraction of X-Rays*, Vol. II, p. 21, B. Bell and Sons, London, 1948.

⁽⁹⁾E. O. Wollan and C. G. Shull, *Phys. Rev.* 73, 830 (1948).

NEUTRON CROSS SECTIONS

factor. For the other expressions the factor σ_{coherent} or $\sigma_{\text{incoherent}}$ is modified to include the corresponding quantities for the different atoms in their relative abundance in the molecule. For an element possessing isotopes but no nuclear spins,

$$\sigma_{\text{coherent}} = 4\pi \left(\sum_k p_k f_k \right)^2, \quad (13)$$

and

$$\sigma_{\text{incoherent}} = 4\pi \left[\sum_k p_k (f_k)^2 - \left(\sum_k p_k f_k \right)^2 \right], \quad (14)$$

where f_k is the scattering amplitude of the k th isotope and p_k is the relative abundance of the k th isotope. For an element possessing nuclear spins, these values, which are more complicated, are given by Halpern, Hamermesh, and Johnson.⁽⁴⁾

Cross-Section Measurements for Nickel. Cross-section measurements were made for normal nickel by using a very fine carbonyl powder. The results of these measurements compared with the calculated curve are shown in Fig. 5.1. The values of the various bound cross sections obtained from these measurements are:

$$\begin{aligned} \sigma_{\text{coherent}} &= 13.1 \text{ barns,} \\ \sigma_{\text{incoherent}} &= 4.8 \text{ barns,} \\ \sigma_{\text{total scattering}} &= 18 \text{ barns,} \\ \theta &= 330^\circ\text{K.} \end{aligned}$$

A comparison of the "measured" and calculated values for the sum of the incoherent and inelastic cross sections is shown in Fig. 5.2. The "measured" values were obtained by subtracting σ_{capture} and $\sigma_{\text{coherent elastic}}$ from the measured total cross section. The capture cross section for nickel was taken as that given by Pomerance,⁽¹⁰⁾ $\sigma_{\text{capture}} = 4.5$ barns at 0.025 ev. The disagree-

ment between the measured values and the values calculated on the basis of the "incoherent approximation" is to be expected, since in this region multiple phonon processes, which are not taken into account by this theory, are undoubtedly occurring. It appears, however, that the "independent oscillator" approximation gives fairly good agreement in this region.

Cross-Section Measurements for Nickel Oxide.

Similar cross-section measurements were made on a nickel oxide sample composed of particles of about the same average size as those in the nickel sample. The average particle diameter was estimated to be between 0.5 and 1 μ . The results of these measurements are shown in Fig. 5.3. A comparison of the measured total cross section with the calculated values is shown in Fig. 5.4. The calculated values in Fig. 5.4 represent

$$\begin{aligned} \sigma_{\text{total}} &= \sigma_{\text{capture}} + \sigma_{\text{incoherent}} \\ &\quad + \sigma_{\text{thermal diffuse}} + \sigma_{\text{coherent elastic}} \\ &\quad + \sigma_{\text{magnetic}} + \text{correction term for small-angle} \\ &\quad \quad \quad \text{scattering not accepted at counter.} \end{aligned}$$

The small-angle correction was determined experimentally to be about 0.75 barn at 3.4 \AA and was assumed to decrease linearly to zero at 1.5 \AA . This approximation is rough but probably not too inaccurate. It is interesting to note that the magnetic-scattering cross section at 3.4 \AA is about 1 barn.

A comparison of the measured and calculated values of the sum of the incoherent and inelastic cross sections is shown in Fig. 5.5. This sum was calculated from both the incoherent approximation and the independent-oscillator approximation. The difference between the calculated and measured values is given in Fig. 5.6. This difference, which can not be satisfactorily explained on the basis of moisture in the sample, amounts to 10% in the total cross section. However, the difference is very large if it is attributed solely to inelastic scattering. At the present time no explanation can be offered for this disagreement and further investigation is contemplated.

⁽¹⁰⁾H. Pomerance, *Phys. Rev.* 83, 641 (1951).

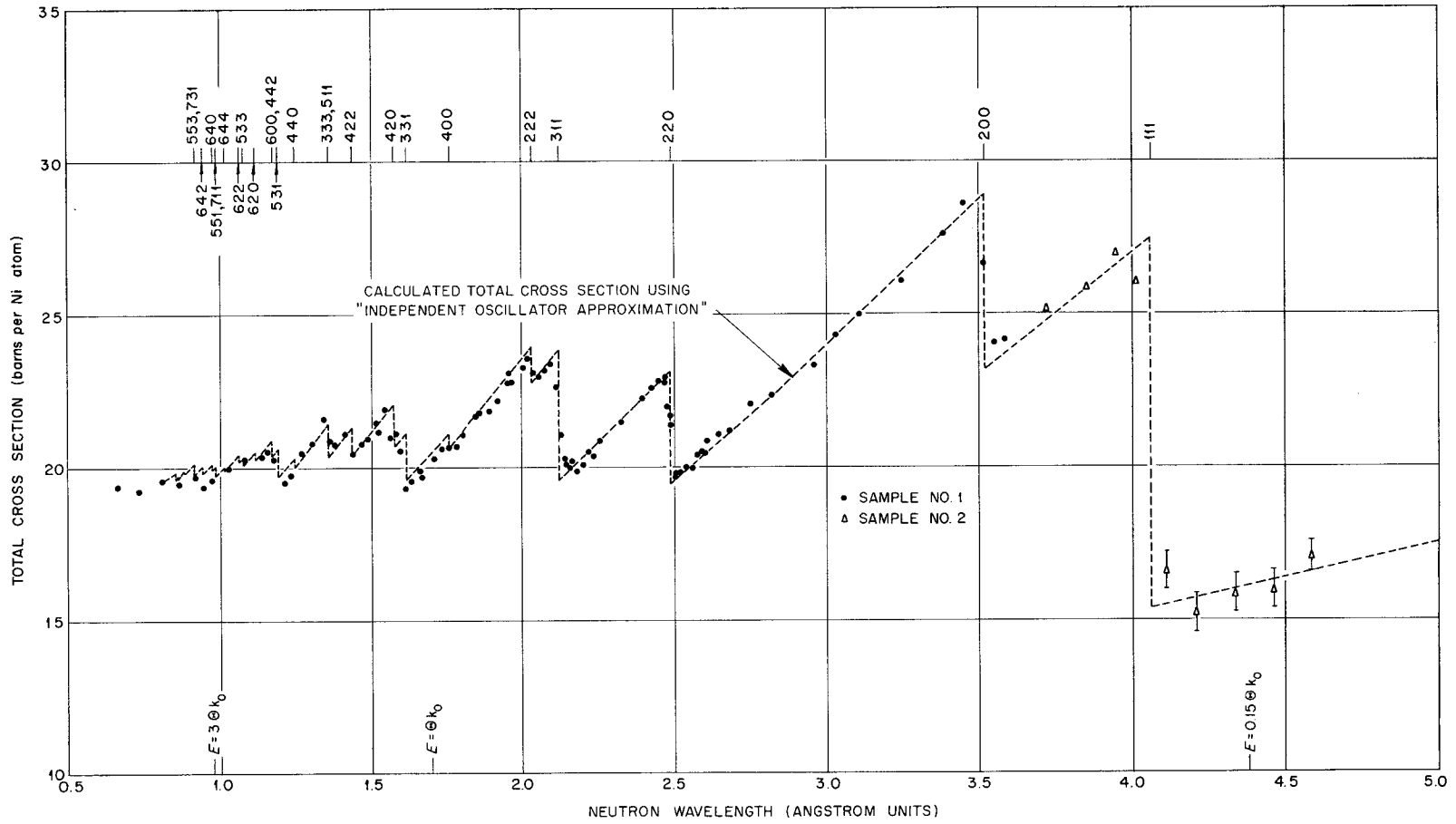


Fig. 5.1. Comparison of the Measured and Calculated Values for the Total Cross Section of Nickel.

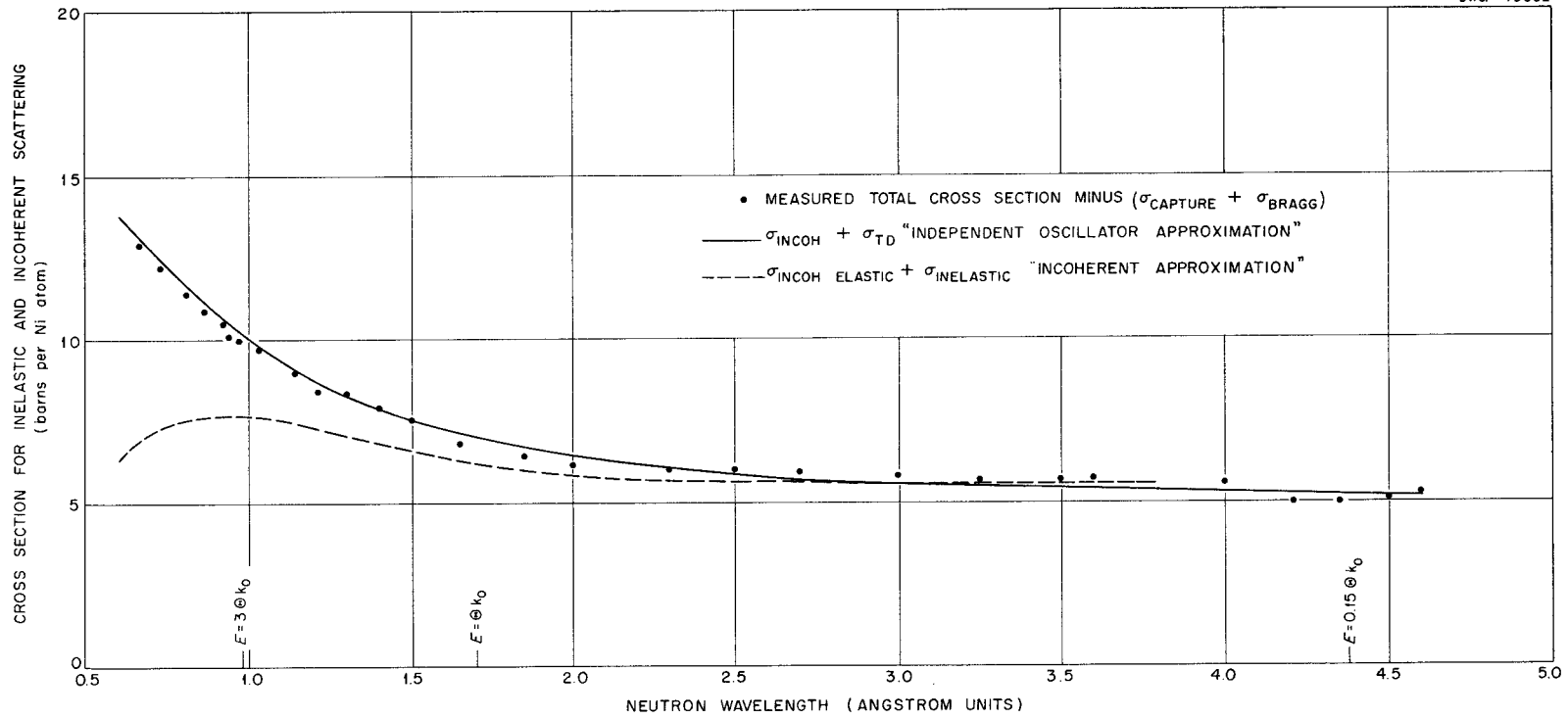
UNCLASSIFIED
DWG. 15052

Fig. 5.2. Inelastic Plus Incoherent Cross Section for Nickel.

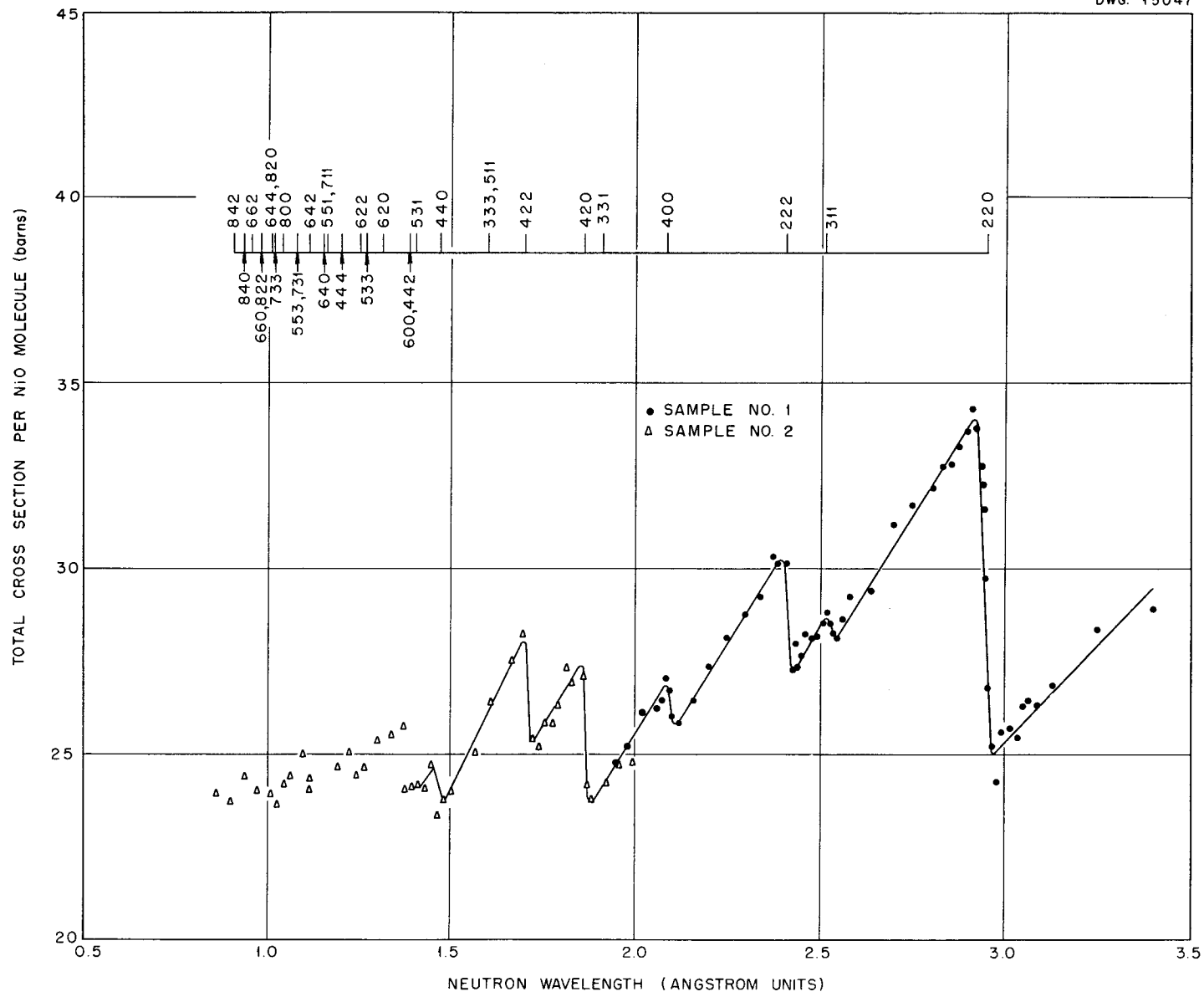


Fig. 5.3. Measured Total Cross Section for Nickel Oxide.

NEUTRON CROSS SECTIONS

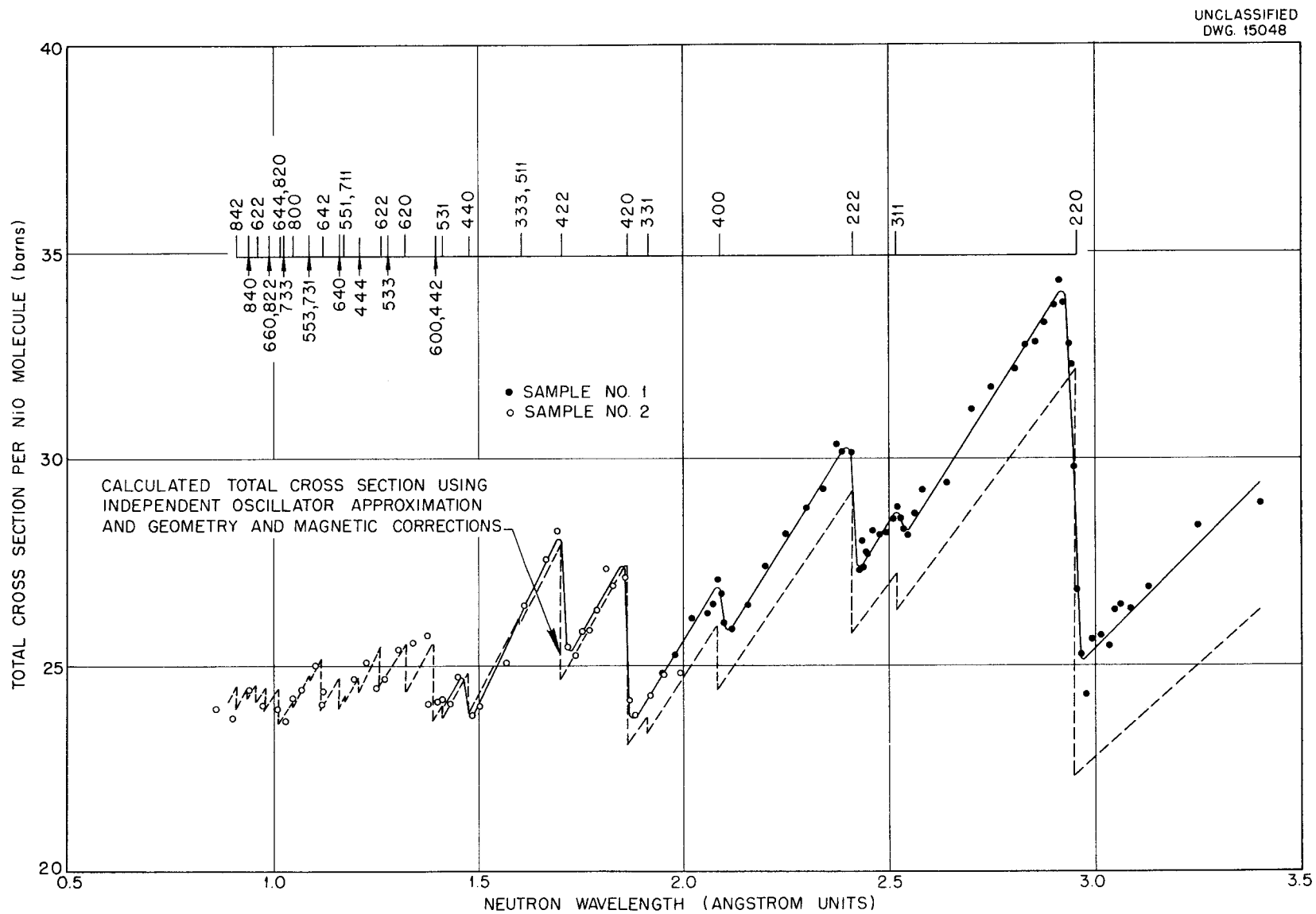


Fig. 5.4. Comparison of the Measured and Calculated Values for the Total Cross Section of Nickel Oxide.

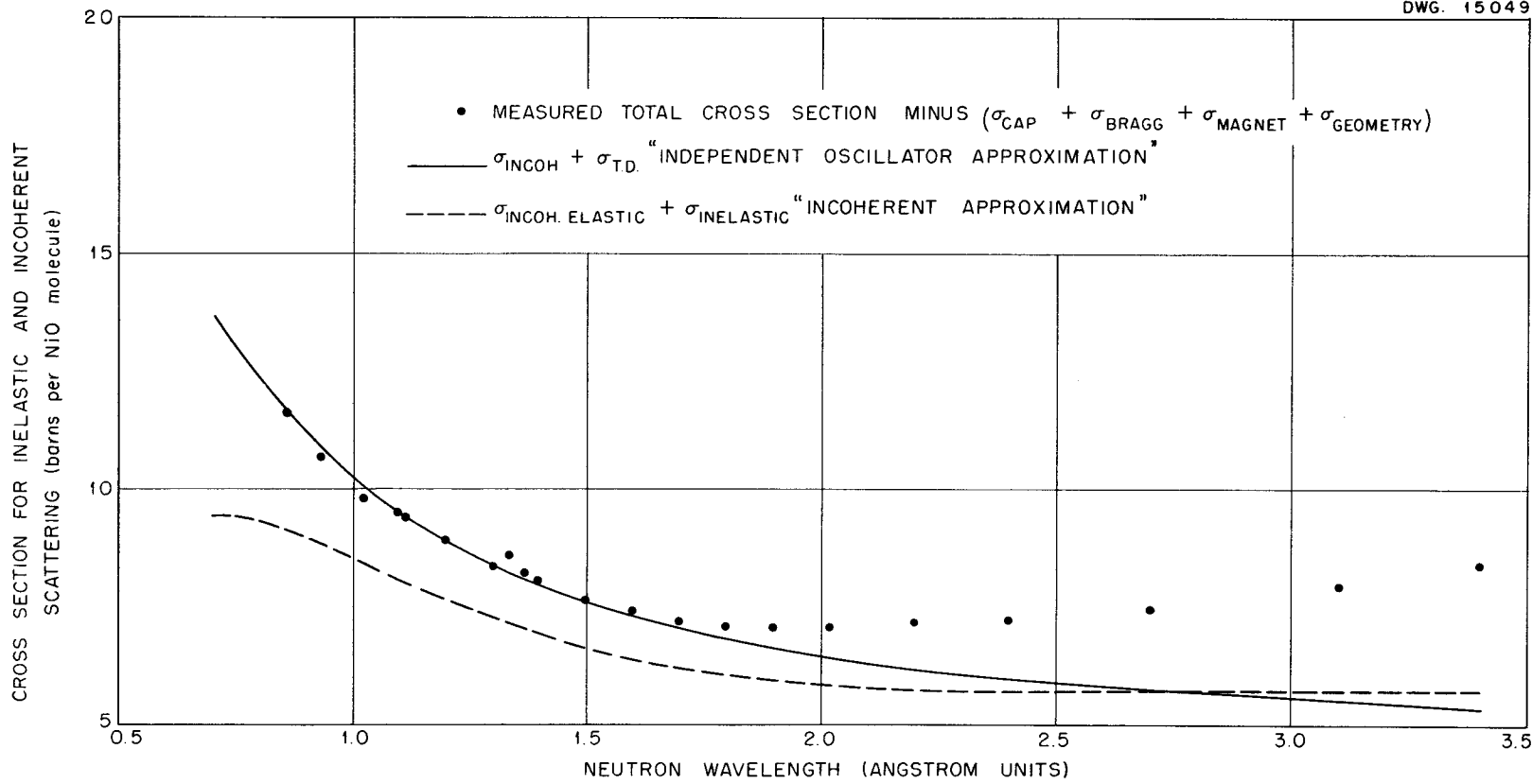


Fig. 5.5. Inelastic Plus Incoherent Cross Section for Nickel Oxide.

NEUTRON CROSS SECTIONS

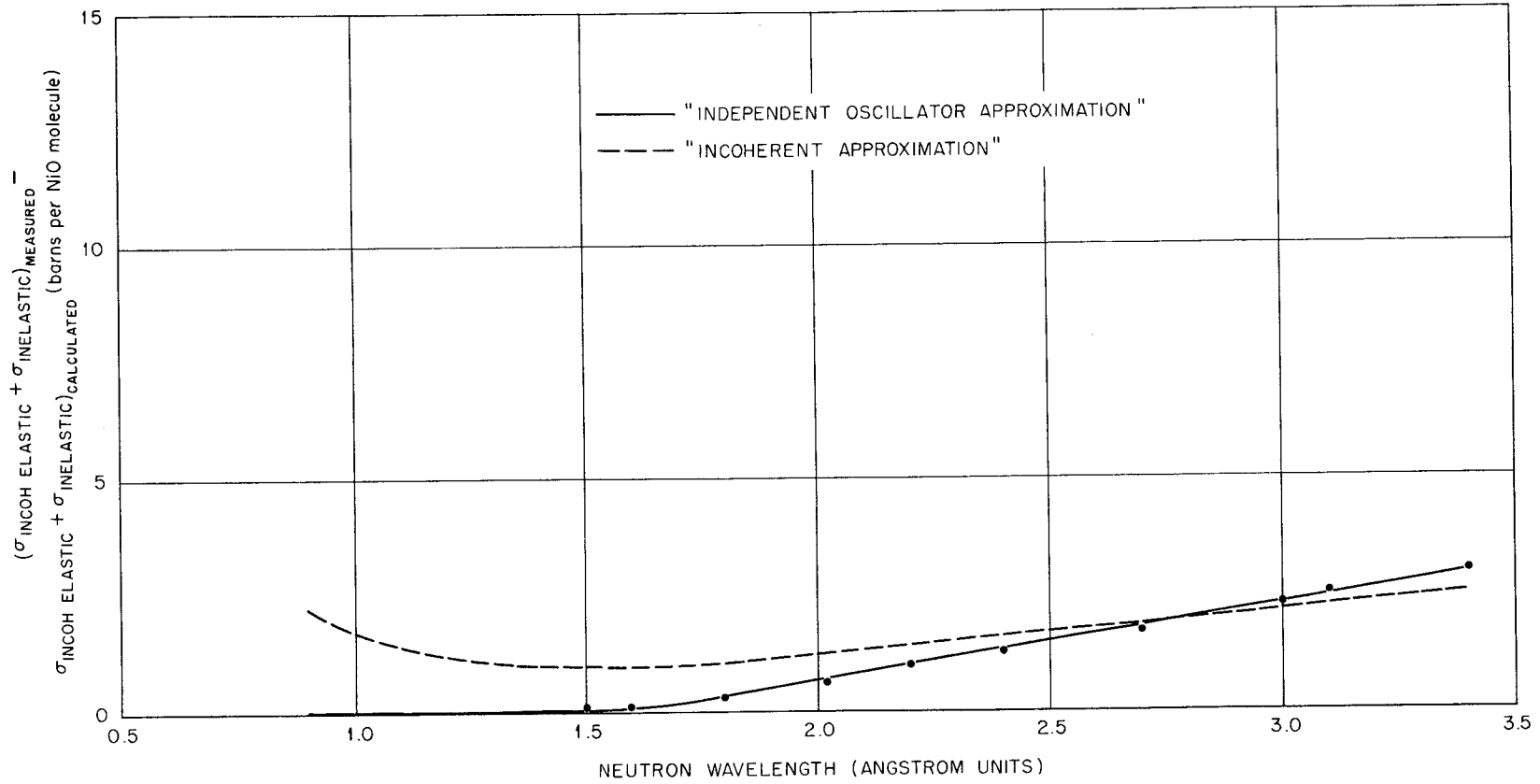
UNCLASSIFIED
DWG. 15550

Fig. 5.6. Difference Between the Measured and Calculated Values for the Incoherent Plus Inelastic Scattering Cross Section of Nickel Oxide.

6. INSTRUMENTATION

CRYSTAL DIODES

P. R. Bell C. Harris
M. Goodrich G. G. Kelley

Crystal diodes have been widely adopted in electronic circuits because of their low forward resistance and small capacitance. Recently some diode characteristics have been observed when a pulse of current (22 ma) is sent through the diode in the forward direction. The low forward resistance is not immediately obtained when the pulse begins; for most diodes the voltage required to produce the current is at first several volts higher than normal and reaches the equilibrium value in approximately $0.1 \mu\text{sec}$. When the current pulse is shut off by applying a back voltage, the diode is quite conductive in the reverse direction. This abnormally large back current may persist for a microsecond. It has been found that most of the present-day diodes are inferior, in these respects, to diodes produced several years ago. The only satisfactory diodes available are recently produced CK707's and old IN34's.

The discovery that both the forward and back resistance are very sensitive to light shining on the diode has caused dismay.

NEUTRON-SENSITIVE SCINTILLATION PHOSPHORS

J. Schenck

The search for better phosphors for detecting and measuring the energy of fast neutrons is continuing. It has recently been discovered that lithium iodide activated with europium (introduced into the mixture in the form of EuCl_2) performs much better than tin-activated lithium iodide. The light output is approximately 40% that of thallium-activated sodium iodide although the time constant for decay of the light flash is longer ($\sim 2.0 \mu\text{sec}$). The light output is approximately a linear function of the particle energy. This can be seen from Fig. 6.1, which shows the pulse spectrum produced by a europium-activated lithium iodide crystal surrounded by paraffin and exposed to a polonium-beryllium source. The peak at 820 pulse-height divisions is the pair peak from the 4.45-Mev gamma ray in C^{12} and should have an energy of

$4.45 - 2mc^2 = 3.43 \text{ Mev}$. The peak at 1130 divisions is that due to the $\text{Li}^6(n,\alpha)\text{H}^3$ reaction, which has a Q value of 4.87 Mev.

The energies shown on the curve are the accepted values and exhibit some departure from linearity; the measured pulse height of the neutron peak is 5% less than that expected from a linear relation. The data for Fig. 6.1 were obtained by interposing some neutron absorber between the source and the detector in order to make the peaks nearly equal. If, instead, a lead absorber is interposed, the neutron peak will be about one hundred times larger than the gamma-ray peak.

The resolution (full width at half maximum) of the neutron peak is about 6%; this corresponds to a neutron energy resolution of about 300 kev.

The phosphor was irradiated with 3-Mev neutrons from the high-voltage Van de Graaff machine,

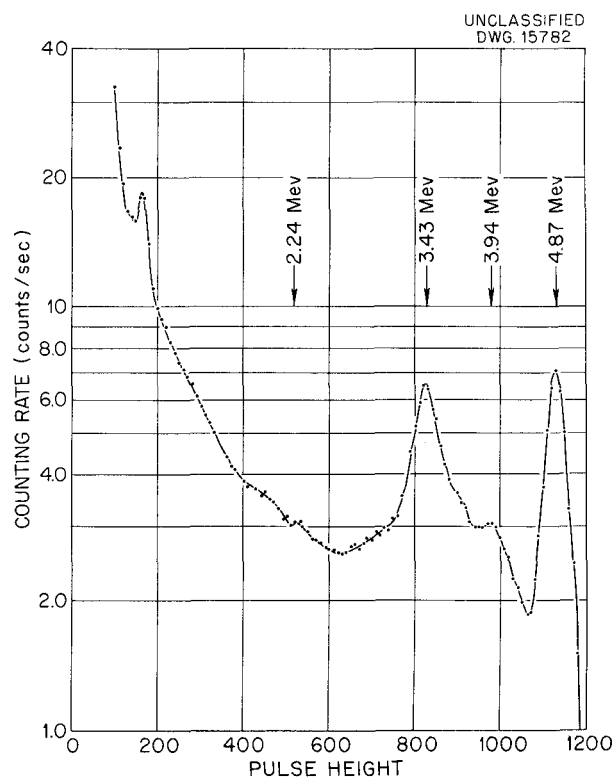


Fig. 6.1. Pulse Spectrum from a Europium-Activated Lithium Iodide Crystal When Exposed to a Moderated Polonium-Beryllium Neutron Source.

THEORETICAL PHYSICS

and a time exposure photograph was taken of the pulses displayed on the face of a cathode-ray tube, Fig. 6.2. The top trace is due to 3-Mev neutrons and the center is due to thermal neutrons. The broad trace at the bottom is probably due to gamma rays. It appears that europium-activated lithium iodide phosphors will be very useful for measuring neutron energies and that interference from capture gamma rays from iodine is not a serious problem. Capture gamma rays may become more troublesome with larger crystals; this could be offset by the use of Li⁶-enriched material.

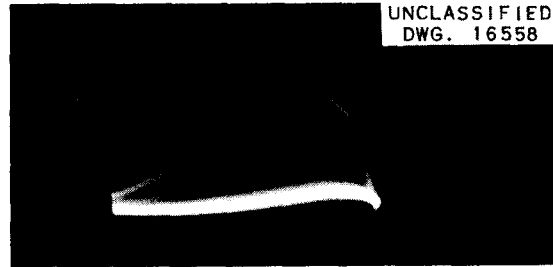


Fig. 6.2. Oscilloscope Photograph of Pulses from a Europium-Activated Lithium Iodide Phosphor Exposed to 3-Mev Neutrons.

7. THEORETICAL PHYSICS

THE PARAMETERIZATION OF QUANTUM ELECTRODYNAMICS

T. A. Welton

The formalism, previously described,⁽¹⁾ for the parameterization of quantum electrodynamics has been further extended. The intent is to produce a theory that allows pair-production but gives no photon self-energy. This is to be accomplished without artificial subtractions (photon self-energy, for example), and an infinite-charge renormalization will be accepted only if its divergence clearly results from something as trivial as the failure of the perturbation theory (as does the divergence of the mass renormalization). Such a theory has been devised by a logical extension of the work previously reported⁽¹⁾ on the parameterization of the one-particle theory.

The parameterized wave equation for a single electron in a specified electromagnetic field is as follows:

$$i\dot{\psi}(x,s) = -i\gamma^\mu \frac{\partial\psi}{\partial x^\mu} + e\gamma^\mu A_\mu \psi . \quad (1)$$

By analogy with the usual second-quantization procedure, Eq. 1 will be taken as the equation of motion for a quantized field variable. The corresponding Schrodinger equation is

$$i\dot{\Psi}(\psi, \bar{\psi}, s) = \left\{ -i \int dx \left(\bar{\psi} \gamma^\mu \frac{\partial\psi}{\partial x^\mu} \right) + e \int dx (\bar{\psi} \gamma^\mu \psi) A_\mu \right\} \Psi , \quad (2)$$

where

$$\bar{\psi} = \tilde{\gamma}^0 \psi^+ ,$$

$$\int dx = \int dx^0 dx^1 dx^2 dx^3 ,$$

$$\dot{F} = \frac{\partial F}{\partial s} .$$

The wave-functional Ψ depends on the values of the field variables $\bar{\psi}$ and ψ at all space-time points. To obtain consistency between Eqs. 1 and 2, the following anticommutation relations must be assumed:

$$[\psi_i(x,s), \psi_k(x',s)]_+ = [\bar{\psi}_i(x,s), \bar{\psi}_k(x',s)]_+ = 0 ,$$

$$[\psi_i(x,s), \bar{\psi}_k(x',s)]_+ = \delta_{ik} \delta(x - x') . \quad (3)$$

The subscripts i and k label the four components of ψ and $\bar{\psi}$.

The formalism is thus far very general and must be specialized by some assumption to describe the "vacuum" state. This will be done by specifying the following vacuum expectation values:

$$\overline{\psi_i(x,s) \psi_k(x',s)} = \overline{\bar{\psi}_i(x,s) \bar{\psi}_k(x',s)} = 0 ,$$

$$\overline{\psi_i(x,s) \bar{\psi}_k(x',s)} = S_{ik}(x, x') , \quad (4)$$

(1) T. A. Welton, *Physics Division Quarterly Progress Report for Period Ending March 20, 1952*, ORNL-1289, p. 39.

where $S_{ik}(x, x')$ is a complicated function depending, in general, on the electromagnetic field. It is a function of $x - x'$ alone, only in the field-free case. Various choices for S_{ik} have been studied by going over to four-momentum space and by taking the field into account only in the lowest order of the perturbation theory.

In the ordinary theory, the vacuum can be taken to correspond to all energy states of the Dirac electron that are empty (one-particle theory), or to all negative energy states that are full and to all positive energy states that are empty (hole theory). The one-particle theory, then, yields an unbelievable electron self-energy, no pair-production, and unbelievable radiative transitions to negative energy levels. The hole theory, on the other hand, leads to plausible (correct to within experimental error) self-energy and pair-production, but produces (to replace the transitions to negative energies) the difficulties of the photon self-energy and the infinite charge renormalization.

Greater freedom is possible in the theory developed here. The possible choices of S_{ik} correspond to taking the following four-momentum states as full:

1. no states,
2. states of negative energy and positive rest mass (equal to the electron mass),
3. states of negative energy and both positive and negative rest mass (equal in magnitude to the electron mass).

There are other possibilities, but they have not yet been studied. Case 1 yields the same results as the parameterized one-particle theory previously described. It predicts the correct electron self-energy and no transitions to negative energies, but gives no positron effects, either "good" or "bad." Case 2 is identical in its predictions with the conventional hole theory. Case 3 is interesting in that it agrees with the hole theory, except in the prediction of no photon self-energy. At the same time, the charge renormalization and Uehling effect vanish identically, together with the low-frequency ($2mc^2$) Delbrück scattering.

The positron theory given by case 3 is regarded as promising, although some refinement *may* be necessary (no clear-cut experiment exists!) to avoid the prediction of the production of two types of electron-positron pairs.

As a means of making the choice between case 2 and case 3, the Lamb shift is being recalculated by the techniques of the parameterized one-particle theory. A very simple procedure has been devised for separating the relativistic and nonrelativistic parts of the calculation, and the work is nearly finished.